Received June 19, 2016, accepted July 8, 2016. Date of publication xxxx 00, 0000, date of current version xxxx 00, 0000.

Digital Object Identifier 10.1109/ACCESS.2016.2593421

Performance of Cognitive Stop-and-Wait Hybrid Automatic Repeat Request in the Face of Imperfect Sensing

ATEEQ UR REHMAN, CHEN DONG, LIE-LIANG YANG, (Fellow, IEEE), AND LAJOS HANZO, (Fellow, IEEE)
School of Electronics and Computer Science, University of Southampton, Southampton SO17 1BJ, U.K.

Corresponding author: L. Hanzo (lh@ecs.soton.ac.uk)

AQ:1 This work was supported in part by the Engineering and Physical Sciences Research Council under Project EP/Noo4558/1 and Project EP/L018659/1, in part by the European Research Council's Advanced Fellow Grant through the Beam-Me-Up Project, and in part by the Royal Society's Wolfson Research Merit Award. The work of A. U. Rehman was supported by the Abdul Wali khan University, Mardan, Pakistan, through the Faculty Development Program.

ABSTRACT The cognitive radio (CR) paradigm has the potential of improving the exploitation of the electromagnetic spectrum by detecting instantaneously unoccupied spectrum slots allocated to primary users (PUs). In order to support the process of spectrum reuse, we consider a CR scheme, which senses and opportunistically accesses a PU's spectrum for communication between a pair of nodes relying on the stop-and-wait hybrid automatic repeat request (SW-HARQ) protocol. This arrangement is represented by the cognitive SW-HARQ (CSW-HARQ), where the availability/unavailability of the PU's channel is modeled as a two-state Markov chain having OFF and ON states, respectively. Once the cognitive user (CU) finds that the PU's channel is available (i.e., in the OFF state), the CU transmits data over the PU channel's spectrum, while relying on the principles of SW-HARQ. We investigate both the throughput and the delay of CSW-HARQ, with a special emphasis on the impact of the various system parameters involved in the scenarios of both perfect and imperfect spectrum sensing. Furthermore, we analyze both the throughput as well as the average packet delay and end-to-end packet delay of the CSW-HARQ system. We propose a pair of analytical approaches: 1) the probability-based and 2) the discrete time Markov chain-based. Closed-form expressions are derived for both the throughput and the delay under the perfect and imperfect sensing environments that are validated by simulation. We demonstrate that the activity of PUs, the transmission reliability of the CU, and the sensing environment have a significant impact on both the throughput and the delay of the CR system.

INDEX TERMS Cognitive radio, primary users, stop-and-wait, HARQ, DTMC, spectrum sensing, imperfect sensing, transmission reliability, throughput, delay, PMF.

LIST OF ACRONYMS

ACK	Positive Acknowledgement
ARQ	Automatic Repeat ReQuest
CD	Correct-detection
CGBN	Cognitive Go-Back-N
CR	Cognitive Radio
CSW	Cognitive Stop and Wait
CU	Cognitive User
DTMC	Discrete Time Markov Chain
FA	False-alarm
FEC	Forward Error Correction
HARQ	Hybrid Automatic Repeat ReQuest
MD	Mis-detection
NACK	Negative Acknowledgement
OFF	Markov chain in OFF state
ON	Markov chain in ON state
PEP	Packet Error Probability
PMF	Probability Mass Function
PR	Primary Radio
PU	Primary User
RS	Reed-Solomon
RTT	Round-Trip Time
SW	Stop and Wait
TS	Time-slot

LIST OF SYMBOLS

α	Transition probability from 'ON' to 'OFF' state
β	Transition probability from 'OFF' to 'ON' state
E	Average
k	Duration for sensing the TS
K_d	Information Bits
λ	Rational Constant
M_c	Total number of packets to be transmitted
M_T	Maximum delay
μ	Real status of the PU's channel
N	Number of packets in a TS
ν	Status of the PU's channel sensed by the CU
N_d	Coded symbols
N_{DP}	Average delay due to busy channel occurring before transmission
$\boldsymbol{P}$	Transition matrix
P_A	Probability that TS is actually free
P_B	Probability that TS is found free due to mis-detection
P_{bs}	Probability of finding a busy TS
$\boldsymbol{P}_d$	PMF of end-to-end delay obtained through simulation
P_e	Packet error probability
P_{fa}	Probability of false-alarm
P_{fr}	Probability of finding a free TS
$P_{i,j}$	$\{i, j\}$th element of the transition matrix
P_{md}	Probability of channel being mis-detected
P_{MF}	Probability distribution of end-to-end packet delay
P_{off}	Probability of the PU's channel being free from the PUs
P_{on}	Probability of the PU's channel being occupied by the PUs
$\boldsymbol{\Phi}$	Steady-state vector
Φ_i	ith element of a steady-state vector
$\boldsymbol{\pi}$	Express steady-state probabilities
π_i	ith element of steady-state vector
$\mathbb{S}$	Sample set
S_i	Represents state i
$\mathbb{S}_N$	Subset of $\mathbb{S}$
$\mathbb{S}_i$	Subset of $\mathbb{S}_N$, which contains states associated with new packets
R_s	Throughput
R'_s	Normalized throughput
R'_S	Simulation throughput
$[\ ]^T$	Transpose of matrix
T	Duration of the TS
T_d	Data transmission epoch
T_D	Total average packet delay obtained from theory
T_{DP}	Delay due to busy channels
T_{DS}	Total average packet delay obtained by simulation
$T_{DS'}$	Normalized average packet delay obtained by simulation
T_p	Duration of packet transmission
T_s	Sensing epoch
T_w	Waiting epoch
τ	Average end-to-end packet delay
τ_s	Average end-to-end packet delay obtained by simulation
ξ	Status of a specific packet
$\mathbf{1}$	Column vector containing 1

I. INTRODUCTION

The 21st century has witnessed an exponential growth in wireless applications, which has significantly increased the electromagnetic spectrum demand and led to spectrum scarcity in the most desirable low-attention frequency bands [1]. In order to identify the cause of the spectrum shortage and to conceive corresponding solutions, the Federal Communication Commission (FCC) in the USA and the European Telecommunications Standards Institute (ETSI) conducted surveys in different parts of the world and at different time instances [2]–[4]. The results of these studies reveal that under the conventional static spectrum allocation policy, substantial segments of the earmarked electromagnetic spectrum are actually under-utilized. For example, the spectrum measurements of [4] demonstrated that the typical spectrum occupancy in the United States varies between 15% to 85%, whereas, the measurements taken in downtown Berkley illustrated in Fig. 1 suggest that the spectrum utilization below 3 GHz is approximately 30%, while in the range of 3–6 GHz is only 0.5% [5], [6]. As a result, the available bandwidth cannot be efficiently exploited, whilst the readily available spectrum remains insufficient for innovative bandwidth-thirsty wireless applications [3], [7]. This inefficient spectrum exploitation motivates the concept of dynamic spectrum access (DSA), which allows the cognitive users (CUs) to access and utilize the unoccupied spectrum holes that have traditionally been exclusively assigned to the primary users (PUs) [7]–[9].

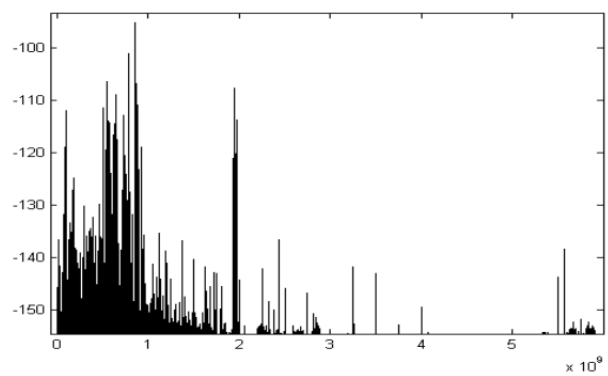

FIGURE 1. Measurement of 0 – 6 GHz spectrum utilization Yang 2005 [5] and Cabric 2007 [6].

The concept of CR system introduced by Mitola and Maguire [10] emerged as a promising paradigm for maximizing the under-utilized spectrum for efficient spectrum utilization, the CUs continuously sense the licensed spectrum with the aim of detecting the unoccupied portions (holes) in the spectrum and then use them for their own

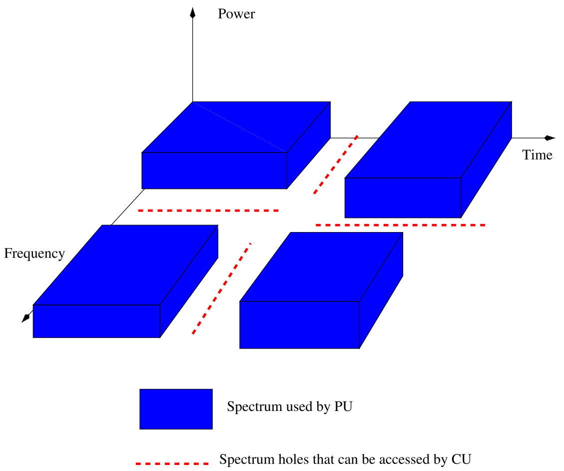

FIGURE 2. An illustration of spectrum hole ©Hossain *et al.* IEEE [7].

data transmission, as shown in Fig. 2 [7], [9], [11]. Moreover, the CU has to relinquish the licensed spectrum as soon as the PRUs wish to access them. In order to improve the exploitation of the licensed spectrum, the regulatory bodies officially allow CUs to access and opportunistically exploit the licensed spectrum. Hence, this concept has been incorporated by various wireless standards, such as IEEE 1900, 802.11y, 802.16h and 802.22, which have been critically appraised in [12].

Automatic Repeat reQuest (ARQ) constitutes an efficient technique of reliable data transmission over noisy channels. The concept of ARQ was originally introduced by Chang [13], which was then classified into three popular ARQ protocols: Stop-and-Wait ARQ (SW-ARQ), Go-Back-N ARQ (GBN-ARQ) and Selective-repeat ARQ (SR-ARQ) [14]–[16]. The principle of ARQ is appealingly simple. After transmitting a packet, if the original transmitter node fails to receive a positive acknowledgement within the defined time duration or if it receives a negative acknowledgement, the packet is retransmitted. The ARQ protocols are capable of achieving reliable data transmission, provided that the channel-induced error rate remains moderate. However, beyond a certain error rate both the throughput and the delay may become inadequate. Hence, for the sake of enhancing the performance, hybrid Forward Error Correction (FEC) and ARQ (HARQ) schemes [17], [18] may be employed. In addition to detecting errors, in HARQ, the FEC scheme also has the capability of correcting a number of errors and the ARQ mechanism is activated for the retransmission of a packet, when residual errors are detected after FEC decoding. As a benefit, HARQ schemes are typically capable of providing a better throughput/delay performance than the corresponding ARQ schemes. Hence, they have been widely used in wireless communication systems [19], [20], which motivated us to study and incorporate the HARQ schemes in CR systems.

Similar to our previous studies [21], [22], we focus our attention on the opportunistic spectrum access in CR systems [7], [9], where a CU senses and occupies a PU's channel for its own transmission, provided that the PU's channel is not occupied at the instant of the demand [23]–[25]. In our studies, the activity of the PU is modelled using a two-state Markov chain, having the 'ON' and 'OFF' states [24], [26], [27]. The channel is considered to be occupied by the PUs in the 'ON' state and to be free in the 'OFF' state. However, when the sensing is unreliable, the Markov chain has four states [22], including the false-alarm and mis-detection events. In this scenario, a time-slot (TS) of duration T is divided into two portions: a sensing epoch (T_s) and a transmission epoch (T_d) [23], [28]. The sensing epoch T_s is used for detecting spectrum holes, while the transmission epoch $T_d = T - T_s$ is used for data transmission. In our CR system, the data transmission relies on the principles of classic stop-and-wait hybrid automatic repeat request (SW-HARQ) [14]–[16].

Our proposed cognitive stop-and-wait (CSW-HARQ) scheme intrinsically amalgamates CR system with the classic SW-HARQ regime in both perfect and imperfect sensing environments. We opted for the SW-HARQ protocol as a benefit of its low complexity at both the transmitter and receiver. However, it wastes time between the end of transmitting a packet and reception of its feedback acknowledgement [14], [15]. Again, in the CSW-HARQ, the CU transmitter first senses a PU's channel and only transmits data if the channel is deemed to be free. Otherwise, it waits until the next TS. After the transmission of a data packet, the transmitter waits for the feedback. At the receiver side, when the CU's receiver receives the packet, it starts its decoding and generates a feedback flag [29], [30]. A positive feedback (ACK) is generated and sent to the transmitter, if an error-free packet is received. Otherwise, a negative feedback (NACK) is generated and sent to the transmitter. Then, the CU transmitter sends a new packet after the reception of an ACK. Otherwise, the previous packet is retransmitted in the next free TS, if it receives a NACK. Based on the above arrangements, we investigate the throughput and delay of the CSW-HARQ scheme both by analysis and by simulation, when assuming either perfect or imperfect sensing.

A. RELATED WORK

Since, the germination of the CR concept, a substantial amount of research has been dedicated to the CR architecture, to its operating principle, spectrum sensing, reconfiguration, spectrum sharing, mobility etc [47], [48]. For instance, the throughput of CR networks has been widely studied in the context of perfectly detecting the activity of the PUs [49], relying on the assumption of the optimal sensing time [23], [26], on cooperative sensing [50] and using the optimal frame length [51]. More particularly, in [23] and [51], the authors have proposed various approaches of maximizing the throughput of the CUs by finding both the optimal sensing duration and the TS duration both in perfect and realistic imperfect sensing scenarios. By contrast, in [28], the trade-off between the sensing duration and throughput has been optimized by proposing a hybrid spectrum sensing and data transmission technique.

Following the spectrum sensing operation, the CUs access the channel for data transmission. The data transmission in CR systems is faced with the usual hostile wireless communication channels, hence powerful error-correction and detection are techniques have been proposed [15], [52]. For example, hybrid automatic repeat request HARQ protocols have been conceived for achieving reliable communication in underwater acoustic networks [37], in satellite communication [53], in audio video transmission over the Internet [54] and in multi-relay environments for transmission over orthogonal TSs [55]. HARQ-aided superposition coding has been proposed for improving the cell-edge coverage, while improving the energy efficiency [56]. The authors of [41], [57], and [58] proposed sophisticated strategies for a multi-component turbo coded HARQ environment where the complexity imposed was reduced by postponing the activation of the turbo iterations until sufficient redundancy was received at the destination. This was also combined with curtailing any further turbo-iterations, when a reliable decision was deemed to be likely. Following that, the authros of [59] proposed channel-adaptive stop-and-wait retransmission schemes in the environment of short-range wireless links for reducing the energy consumption as compared to the classic SW retransmission schemes. Moreover, HARQ has also been involved in various IEEE standards [60]–[62]. Some of the related studies are presented at a glance in Fig. 3.

There is a paucity of studies on the analysis of ARQ protocols in the context of CR. Based on our observations, the dynamic nature of PUs makes the analytical modelling of the ARQ protocols in the context of CR more challenging. The studies performed in this direction include [29], [66], [67], and [69]–[81]. However, these studies do not provide the complete theoretical throughput and delay analysis of the CR system employing ARQ protocols. Specifically, in [69]–[71], the CUs sense the presence of the PUs by listening to their ARQ feedback. However, the authors did not investigate the performance of CUs using ARQ techniques. The throughput of the selective-repeat ARQ protocol evaluated in the context of CR systems has been studied in [66], where an efficient resource allocation scheme has been proposed for multi-hop relaying systems. Then, the authors of [29] and [72] have performed the seminal analysis of ARQ-aided relay-assisted CR systems. Moreover, the authors of [76] analyzed the performance of spectrum sharing networks using HARQ feedback in terms of the attainable throughput and outage probability. Following that, in [77] the efficiency of data transmission was studied in the context of finite-length codewords in spectrum sharing networks.

The authors of [73] and [74] have proposed an improved HARQ scheme employing an anti-jamming coding approach for achieving reliable communication in CR systems. As a further development, a network coding assisted ARQ scheme has been proposed in [75], which aims for improving the efficiency of the conventional ARQ schemes. A hybrid of the spectrum interweave and underlay sharing paradigms has been proposed in [78] and [79] for improving the performance of the CU. The authors of [79] have also involved ARQ for improving the attainable reliability. Moreover, in [82] energy-efficient dynamic spectrum access protocols were proposed for CR nodes in order to enhance the overall channel utilization without affecting the performance of the PU. On the other hand, the authors of [67], [80], and [81] comprehensively surveyed the various techniques employed in the context of CR systems.

B. CONTRIBUTION AND PAPER STRUCTURE

This paper constitutes an evaluation of our prior contributions [21], [22], in which we studied both the throughput and delay of CSW-HARQ, and of cognitive Go-Back-N (CGBN) HARQ in the context of a CR system. Particularly, in [22] a simulation based study was provided for characterizing the performance of CGBN-HARQ in both perfect and in imperfect sensing environments. However, in this contribution, we extend the work presented in [21] to the imperfect sensing environment and derived closed-form analytical expressions. It is observed that the respective parameters have to be carefully adapted according to the specific communication environment considered for maximizing the throughput and for minimizing the delay of the system. Against the above background, the contributions of this paper can be summarized as follows:

(a) The proposed CSW-HARQ scheme intrinsically amalgamates the CR capability with the conventional SW-HARQ protocol in order to achieve reliable data transmission in realistic imperfect sensing. Our protocol enables the CR transmitter to sense the channel before using it and to receive feedback at all times, regardless of the PUs activity.

(b) Firstly, the CSW-HARQ scheme is modelled and theoretically analysed using a probability-based approach considering both perfect and imperfect reusing. Using this approach, closed-form expressions are derived for the a) average packet delay, b) for the throughput of the CU system and c) for the end-to-end packet delay. Both the probability distribution and the average of the end-to-end packet delay are formulated.

(c) Secondly, based on Discrete Time Markov Chain (DTMC) approach, closed-form expressions are derived for the a) throughput of the CU system b) for the average packet delay and c) for the end-to-end packet delay, including its probability distribution and average end-to-end packet delay.

(d) Finally, we validate theoretical results by simulations.

The rest of this paper is organized as follows. We model CR system considered in Section II. The basic principles of the proposed CSW-HARQ transmission scheme are discussed in Section III, followed by the operation of the CU transmitter and receiver in Sections III-A and III-B, respectively. In Section IV and V, a probability-based approach as well as

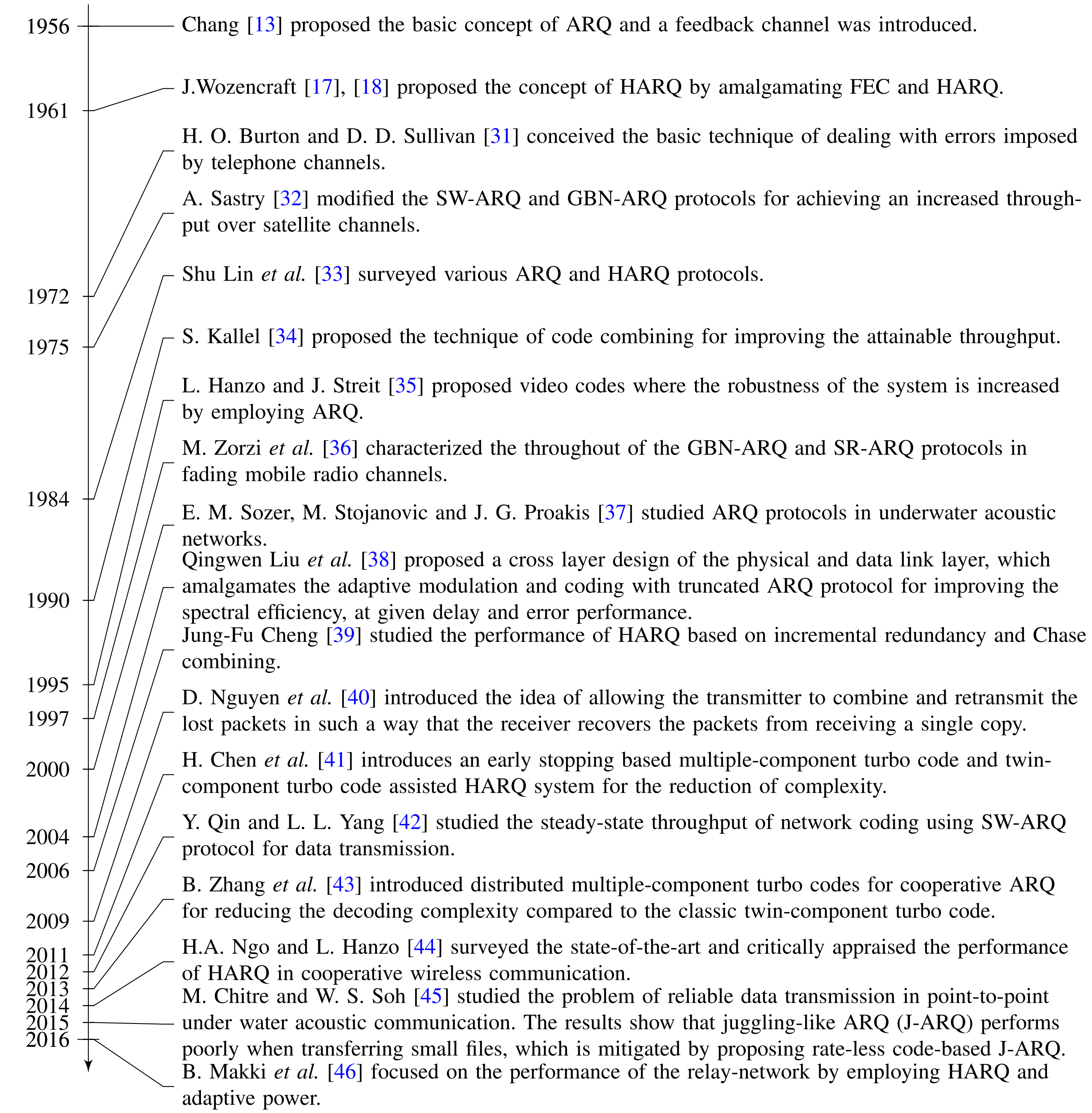

FIGURE 3. Timeline of HARQ in wireless communication.

a Markov chain-based approach are provided, while our and the performance results are discussed in Section VI. Finally, our conclusions are summarized in Section VII.

II. SYSTEM MODEL

In this section, we describe both the primary radio (PR) and the CR systems, as well as the assumptions invoked in our analysis and for obtaining the results of Section VI.

A. MODELING THE PRIMARY USER

As in [22], we assume that there is a PU's channel, which is sensed and used by the CR system considered. We assume that the PUs become active during each TS of duration T independently with the same probability. Specifically, the activation of the PU's channel by the PUs is modeled as a two-state Markov chain having the state transitions shown in Fig. 6. The state 'OFF' represents that the channel is free for the CU to use, whereas the state 'ON' indicates that the channel is

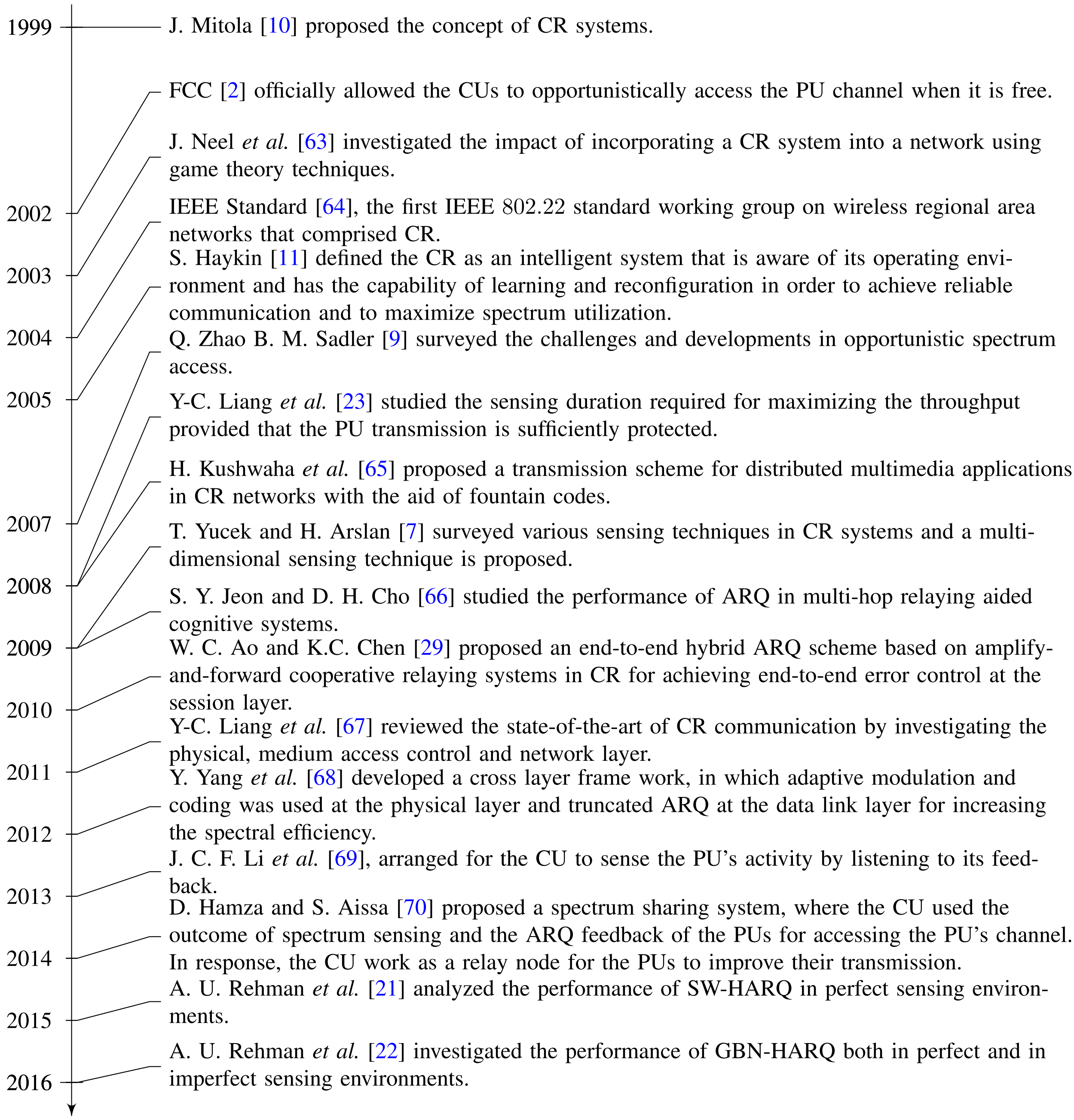

FIGURE 4. Timeline of cognitive radio in the context of HARQ.

occupied by the PUs; α and β represent the transition probabilities from the 'OFF' and ON' to the 'ON' and 'OFF' state, respectively. Let the probabilities of the PUs channel being in the 'ON' and 'OFF' states be P_{on} and P_{off}, respectively. Then, it can be readily shown that if the Markov chain is in its steady state, we have [14]

$$P_{on}\alpha = P_{off}\beta, \tag{1}$$

and from $P_{off} = 1 - P_{on}$ we have:

$$P_{on} = \frac{\beta}{\alpha+\beta}, \quad P_{off} = \frac{\alpha}{\alpha+\beta}. \tag{2}$$

Furthermore, as shown in Fig. 7(a), we assume that if the PU's channel is found in the 'ON' state at the start of a TS, it remains in the 'ON' state until the end of that TS, and using this TS should be avoided by the CU. On the other hand, if a TS is deemed to be free from the PUs, then the CU may use it [26].

B. MODELING THE COGNITIVE USER

In the CR system, each TS of duration T is divided into two phases: the sensing duration of T_s seconds and the data transmission duration of $T_d = T - T_s$ seconds, as shown

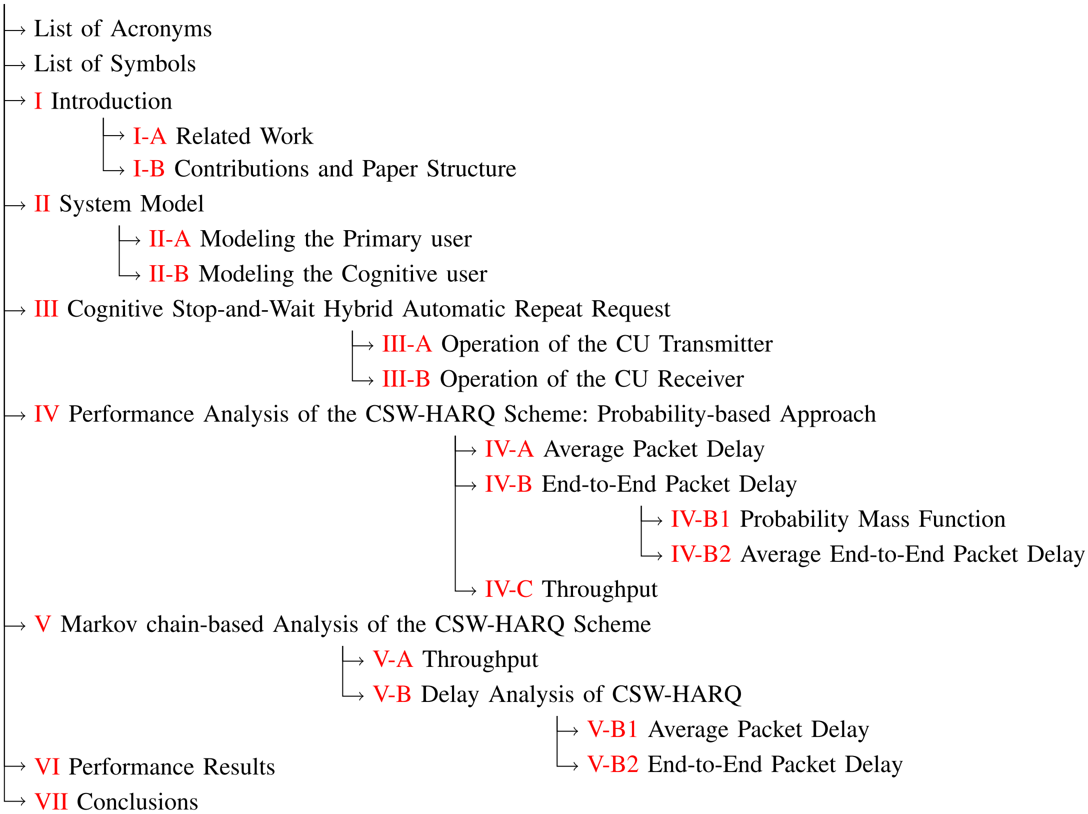

FIGURE 5. **The structure of this paper.**

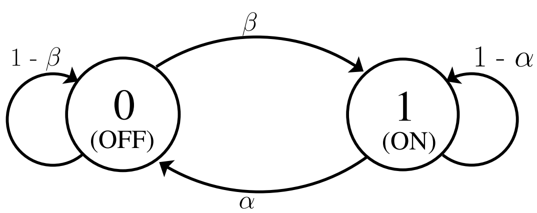

FIGURE 6. **Two-state discrete-time Markov chain model of the PU system.**

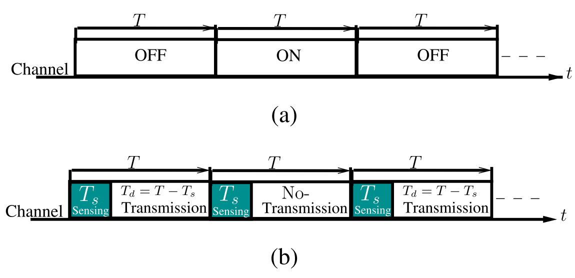

FIGURE 7. **Time-slot structure of PU and CU, where a CU TS consists of a sensing duration of T_s and a transmission duration of $T_d = T - T_s$, when given the total duration T of a time-slot. (a) Pattern of channel usage by PU. (b) Pattern of channel usage by CU.**

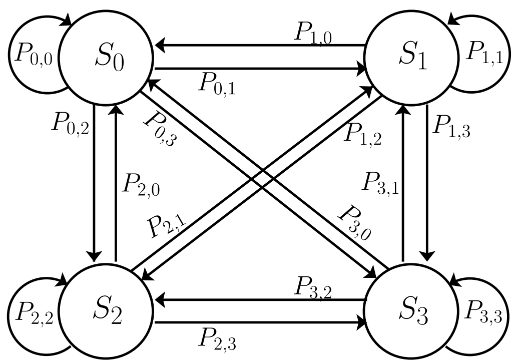

FIGURE 8. **Discrete-time Markov chain modeling of the CR system. In state S_0 = 00, the channel is sensed free when given that it is free; S_1 = 01, the channel is sensed busy when given that it is free. Similarly, the states S_2 = 10 and S_3 = 11 are defined.**

in Fig. 7(b). When the PU's channel is deemed to be 'OFF' within the sensing period T_s, the CR system can use the time T_d for its data transmission based on the principles of CSW-HARQ. However, the sensing decision of the PU's channel may be imperfect, hence resulting in false-alarm, when the channel is 'OFF', but detected to be 'ON'. Alternatively, mis-detection is encountered when the PU's channel is 'ON', but detected to be 'OFF'. In summary, the transitions are shown in Fig. 8. Correspondingly,

$$\boldsymbol{P} = \begin{bmatrix} P_{0,0} & P_{0,1} & P_{0,2} & P_{0,3} \\ P_{1,0} & P_{1,1} & P_{1,2} & P_{1,3} \\ P_{2,0} & P_{2,1} & P_{2,2} & P_{2,3} \\ P_{3,0} & P_{3,1} & P_{3,2} & P_{3,3} \end{bmatrix}. \quad (3)$$

Let the false-alarm and mis-detection probabilities be expressed as P_{fa} and P_{md}, respectively. Then from Fig. 8, we obtain

$$\begin{aligned}
P_{0,0} &= P_{1,0} = (1-\beta)(1-P_{fa}) \\
P_{0,1} &= P_{1,1} = (1-\beta)P_{fa} \\
P_{0,2} &= P_{1,2} = \beta P_{md} \\
P_{0,3} &= P_{1,3} = \beta(1-P_{md}) \\
P_{2,0} &= P_{3,0} = \alpha(1-P_{fa}) \\
P_{2,1} &= P_{3,1} = \alpha(1-P_{fa}) \\
P_{2,2} &= P_{3,2} = (1-\alpha)P_{md} \\
P_{2,3} &= P_{3,3} = (1-\alpha)(1-P_{md}). \qquad (4)
\end{aligned}$$

Furthermore, let the steady state probabilities of the Markov chain be expressed as $\mathbf{\Phi} = [\Phi_0, \Phi_1, \Phi_2, \Phi_3]^T$. Then, we have [14], [83]

$$\mathbf{\Phi} = \boldsymbol{P}^T \mathbf{\Phi}. \qquad (5)$$

Explicitly, $\mathbf{\Phi}$ is the right eigenvector of $\mathbf{P}^T$ associated with an eigenvalue of 1. Therefore, when substituting the items in (4) into (3) and solving Equation (5), we obtain

$$\begin{aligned}
\mathbf{\Phi} &= [\Phi_0 \quad \Phi_1 \quad \Phi_2 \quad \Phi_3]^T \\
&= \lambda \times \left[\frac{\alpha(1-P_{fa})}{\beta(1-P_{md})} \quad \frac{\alpha(P_{fa})}{\beta(1-P_{md})} \quad \frac{(P_{md})}{(1-P_{md})} \quad 1 \right]^T, \qquad (6)
\end{aligned}$$

where $\lambda \in \mathbb{R}$. Upon exploiting the property of

$$\sum_{i=0}^{3} \Phi_i = 1, \qquad (7)$$

gives

$$\lambda = \frac{\beta(1-P_{md})}{\alpha+\beta}. \qquad (8)$$

Consequently, the steady state probabilities of the CR system in the state S_0, S_1, S_2 and S_3 are

$$\begin{aligned}
\Phi_0 &= \frac{\alpha(1-P_{fa})}{\alpha+\beta}, \quad \Phi_1 = \frac{\alpha P_{fa}}{\alpha+\beta}, \\
\Phi_2 &= \frac{\beta P_{md}}{\alpha+\beta}, \quad \Phi_3 = \frac{\beta(1-P_{md})}{\alpha+\beta}. \qquad (9)
\end{aligned}$$

III. COGNITIVE STOP-AND-WAIT HYBRID AUTOMATIC REPEAT REQUEST

In our CSW-HARQ system, data are encoded using a Reed-Solomon (RS) code RS(N_d, K_d) [15], defined over the Galois Field of GF(q)=GF(2^m), where K_d and N_d represent the number of information and coded symbols, respectively, and m is the number of bits per symbol. We assume that every packet consists of a RS codeword, which is transmitted within T_p seconds. Let $N = T_d/T_p$. Then, within a free TS, the CU transmitter can transmit a packet using the T_p seconds and then waits for the feedback. We assume that the RS code is capable of correcting upto t random symbol errors and can ideally detect the uncorrectable errors, which is time for sufficiently long codes.

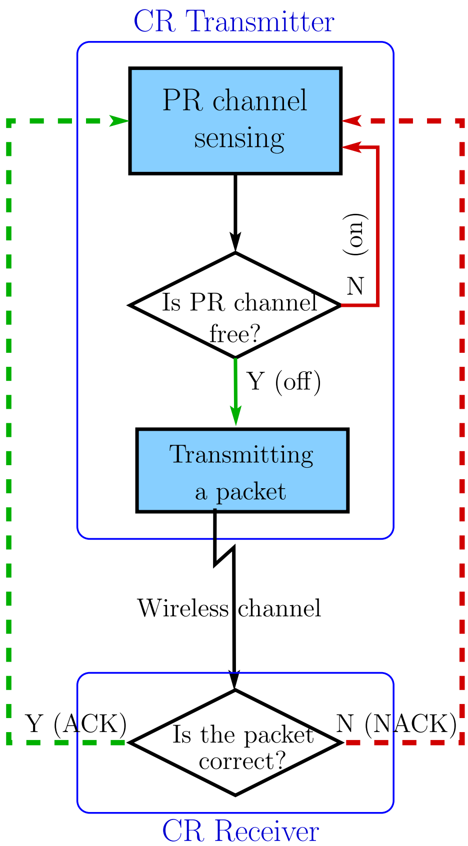

FIGURE 9. Flow chart showing the operations of the proposed CSW-HARQ scheme.

Given the above assumptions, data are transmitted between a pair of CUs over the PU channel based on the principles of our CSW-HARQ scheme, which is characterized in Fig. 9 and formally stated in Algorithm 1, as detailed below. For clarity, Algorithm 1 is divided into two parts, namely the transmitter part and the receiver part. The transmitter always senses the PR channel and (re)transmits a packet, when the channel is free from PRUs. On the other hand, at the receiver side, RS decoding and error correction is performed, based on which a feedback signal is generated for the received packet. We assume that the receiver has perfect knowledge concerning the success or failure of decoding and updates its buffer accordingly.

A. OPERATION OF THE CU TRANSMITTER

In the classic SW-HARQ, the transmitter sends a single packet in a TS and then waits for its feedback, which is expected to be received after a specified round-trip time (RTT). By contrast, in the CSW-HARQ, the CU transmitter first has to sense the PU's channel before the transmission or retransmission of a packet. If the PU channel is correctly detected to be 'OFF', or when the PU channel is mis-detected as being 'OFF' state when it is actually 'ON', the CU transmitter transmits a packet. Otherwise, if the PU channel is correctly sensed to be 'ON' or when it is falsely

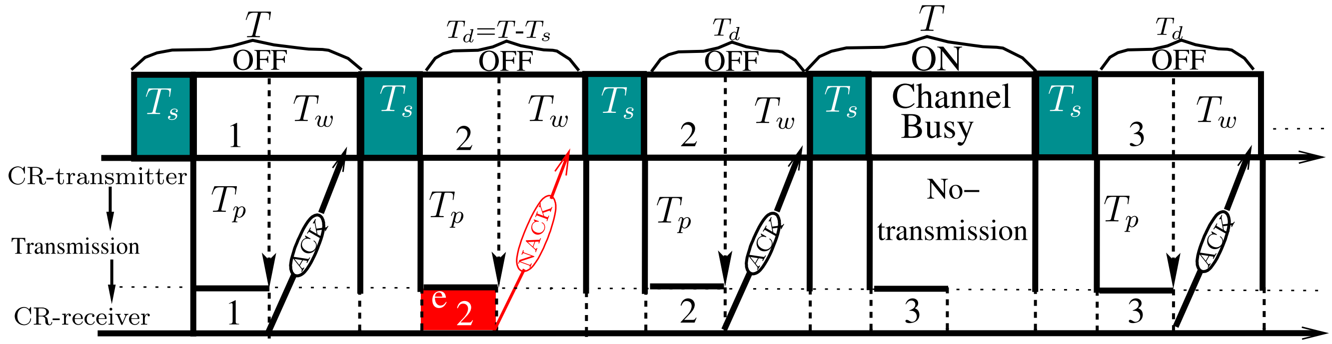

FIGURE 10. The transmission flow of the proposed CSW-HARQ scheme. The total duration of each time-slot is $T = T_s + T_d$, where T_d consists of a packet's transmission duration and its waiting epoch T_w.

Algorithm 1 CSW-HARQ Algorithm

Initialization: M_c = number of packets, $T_d = N$, $T_s = k$, $i = 1$, TS= 1.
Input: T_d, T_s, packets.
while $i \leq M_c$ **do**
  CU transmitter senses a time-slot (TS).
  if TS is free and no false-alarm **OR** TS is busy but mis-detected **then**
    transmits the ith packet and, then,
    waits for T_w duration to receive feedback.
    if the ith packet is received error-free **then**
      receiver sends ACK signal.
      $i = i + 1$.
    else
      receiver sends NACK. It could be because of
      mis-detection or channel noise.
    end if
  else
    The TS may be found busy due to correct detection or false-alarm,
    hence, the transmitter waits until the next TS.
  end if
  TS=TS+1.
end while

detected to be 'ON', while it is actually 'OFF', then the transmitter has to wait until the next TS and has to sense the channel again. The CSW-HARQ operations are summarized both in the Algorithm 1 and in Fig. 9. Similar to the classic SW-HARQ scheme, the CU transmitter in CSW-HARQ has a buffer of size one, which is updated based on the feedback flag of each transmitted packet.

We assume that all the packets are of the same length and that the CU transmitter is always ready to transmit these packets, provided that there are free TSs. As shown in Fig. 10, each CU packet consists of a RS coded codeword, which is transmitted within the duration of T_p seconds. After transmitting a packet, the CU transmitter waits for a duration of T_w seconds in order to receive its feedback. We assume that the RTT is T_d, which is the time interval between the transmission of a packet, and the instant when its feedback acknowledgement is received. Therefore, in our CSW-HARQ scheme, the feedback flag of each packet should be received within the RTT duration of T_d, as shown in Fig. 10. Specifically, if a positive feedback (i.e., ACK) of a packet is received by the CU transmitter within the RTT, this packet is then deleted from the transmitter's buffer and a new packet is transmitted in the next free TS which is also stored in the transmitter buffer. However, if a NACK is received, then the transmitter retransmits the erroneous packet in the next free TS. It is worth mentioning that, when there is a mis-detection of the PU channel, the packet transmitted will become erroneous with a high probability, due to collision with the PU's transmitted signals. On the other hand, when there is a false-alarm, the CU will not transmit, even though the PU channel is free, which results in a reduced throughput.

B. OPERATION OF THE CU RECEIVER

When the CU receiver receives a packet from the CU transmitter, it invokes RS error-correction/detection and then generates a feedback flag accordingly. Specifically, if a packet is correctly recovered by the RS decoder, an ACK signal is fed back to the CU transmitter. Otherwise, a NACK signal is sent to the CU transmitter in order to request a retransmission. In this paper, we assume that the feedback channel is perfect and that the receiver has a buffer size of one packet, which is updated only when a packet is correctly received [14]–[16].

IV. PERFORMANCE ANALYSIS OF THE CSW-HARQ SCHEME: PROBABILITY-BASED APPROACH

In this and the next sections, we analyze the performance of the proposed CSW-HARQ scheme. We consider three performance metrics, namely, 1) the Average packet delay; 2) the End-to-end packet delay; and 3) the Throughput. They are defined as follows. **Average packet delay**: the average number of TSs (or T_p's) required for the successful transmission of a packet. **End-to-end packet delay**: the average time duration from the first transmission of a packet to the instant when it is finally successfully received.

Throughput: the error-free transmission rate of the CR system [15], [42].

In this paper, we introduce two approaches in our analysis, which are the probability-based approach employed in this section, and the discrete time Markov chain (DTMC)-based approach employed in Section V. Our analytical approaches will be validated in Section VI by comparing the results obtained from the numerical evaluation of the derived formulas with those obtained from simulations. Let us first use the probability-based analysis to analyze the average packet delay.

A. AVERAGE PACKET DELAY

In the traditional SW-HARQ scheme, the delay is generated by the data transmitted over unreliable channels, which results in erroneous transmission and thereby requires retransmission, in addition to the basic transmission delay. In our proposed CSW-HARQ scheme, the unreliable channels also introduce delay similarly to the traditional SW-HARQ. Furthermore, in the CSW-HARQ, there is an extra delay both owing to the unavailability and due to the false detection of the PU's channel. In order to analyze the packet delay of the CSW-HARQ scheme, let us denote the average delay due to the busy PU's channels as T_{DP}. It can be shown that the PU's channel is found busy in the following two scenarios:

(a) The PU channel is 'ON' state and the state is correctly detected.
(b) The PU channel is 'OFF', but false-alarm occurs, resulting in the CU not using the channel.

Therefore, according to the definitions in Section II-B, the probability that the CU finds that a TS is busy can be expressed as

$$P_{bs} = P_{on} \cdot (1 - P_{md}) + P_{off} \cdot P_{fa}, \tag{10}$$
$$= \frac{\beta(1 - P_{md})}{\alpha + \beta} + \frac{\alpha P_{fa}}{\alpha + \beta},$$
$$= \frac{1}{\alpha + \beta}\big[\beta(1 - P_{md}) + \alpha P_{fa}\big]. \tag{11}$$

On the other hand, there are only two scenarios for the CU to access the PU's channel for its own transmission:

(a) The PU's channel is in the 'OFF' state, which is correctly detected by the CU.
(b) The PU's channel is in the 'ON' state, but it is mis-detected by the CU.

Correspondingly, the probability of the above events can be expressed as

$$P_{fr} = P_{off} \cdot (1 - P_{fa}) + P_{on} \cdot P_{md}, \tag{12}$$
$$= \frac{1}{\alpha + \beta}\big[\alpha(1 - P_{fa}) + \beta P_{md}\big]. \tag{13}$$

Explicitly, we have $P_{fr} = 1 - P_{bs}$. Moreover, let $T_{DP}(i)$ be defined as the delay imposed by $(i-1)$ busy TSs prior to a free TS, yielding

$$T_{DP}(i) = (i-1)T. \tag{14}$$

Then, the average delay T_{DP} required by the CU to find a free TS may be formulated as

$$\begin{aligned} T_{DP} &= E\left[T_{DP}(i)\right] = E\left[(i-1)T\right] \\ &= \sum_{i=1}^{\infty}(i-1)TP_{bs}^{i-1}P_{fr} \\ &= \frac{(P_{bs} \cdot P_{fr})T}{(1-P_{bs})^2} = \frac{P_{bs}T}{(1-P_{bs})}, \\ &= \frac{\alpha P_{fa} + \beta(1-P_{md})}{\alpha(1-P_{fa}) + \beta P_{md}} \cdot T. \end{aligned} \tag{15}$$

Let us assume that a packet is transmitted over a TS that is supposed to be free, but a delay is introduced by transmission over an unreliable channel. If a packet is successfully delivered in the first attempt, it induces a delay of a T/T_p seconds. By contrast, each retransmission will impose a delay of T seconds. As the analysis of Section IV-A shows, erroneous transmissions may take place in the actually free TSs, or in busy TSs misclassified by the from CU transmitter. Let $T_D(i)$ denote the delay given by the event that the CU transmitter uses a total of i transmissions for successfully delivering a packet to the CU receiver. Here, $T_D(i)$ includes both the delay imposed by finding free TSs and the delay due to the packet's transmission. Furthermore, some of the TSs are free and correctly sensed by the CU system, while others are actually busy TSs but they may be mis-detected by the CU. Therefore, given that a free TS is identified by the CU, the probability that the TS is actually free can be expressed as

$$P_A = \frac{P_{off}(1 - P_{fa})}{P_{fr}}. \tag{16}$$

By contrast, given that a free TS is discovered by the CU, the probability that it is resulted from a mis-detection is

$$P_B = \frac{P_{on}P_{md}}{P_{fr}}. \tag{17}$$

Remembering that each transmission attempt requires an average time of T_{DP} seconds for finding a free TS, plus a subsequent delay of T seconds for the actual round trip transmission, we hence have,

$$T_D(i) = i(T + T_{DP}), \tag{18}$$

when i transmissions are used for the successfully delivery of a single packet. According to the principles of the CSW-HARQ, the transmitter sends a packet in each free TS. Hence, the average packet delay T_D can be evaluated by

$$T_D = \frac{1}{N}E\left[T_D(i)\right] = \frac{1}{N}E\left[i(T + T_{DP})\right], \tag{19}$$

where the multiplier $1/N$ is because each packet is transmitted within N packet durations. Let us denote the packet error probability (PEP) for the packets sent in the free TSs by P_e, after RS decoding. We assume that the PEP of those packets that were transmitted because of mis-detection in the busy

TSs is as high as one. Then, it can be shown that we have

$$\begin{aligned}
T_D &= \sum_{i=1}^{\infty}\sum_{j=0}^{i-1} i(T+T_{DP})\binom{i-1}{j}(P_B)^j\cdot(P_A)^{i-j}\\
&\quad\cdot(P_e)^{i-j-1}(1-P_e)\\
&= \frac{T}{N}(1+N_{DP})\Bigg(\sum_{i=1}^{\infty}\sum_{j=0}^{i-1}\binom{i-1}{j} i(P_B)^j(P_A)^{i-j}\\
&\qquad\cdot(P_e)^{i-j-1}(1-P_e)\Bigg)\\
&= \frac{T}{N}\left(\frac{P_A(1-P_e)(1+N_{DP})}{(P_B+P_AP_e-1)^2}\right)\text{ (seconds)} \qquad (20)
\end{aligned}$$

where $N_{DP} = T_{DP}/T$. Moreover, after normalizing the average packet delay T_D using the packet duration T_p, T_D can be expressed as

$$T_D = \left(\frac{k+N}{N}\right)\left(\frac{P_A(1-P_e)(1+N_{DP})}{(P_B+P_AP_e-1)^2}\right)T_p's, \qquad (21)$$

where $T = (k+N)T_p$ is applied.

B. END-TO-END PACKET DELAY

In this section, we derive the probability mass function (PMF) of the end-to-end packet delay, as well as the average end-to-end packet delay. Here the end-to-end delay of a packet represents the time duration spanning from the first transmission of the packet to the time that the packet is successfully received.

1) PROBABILITY MASS FUNCTION

First, it is worth restating that the delay between the first transmission and the final error-free reception of a packet depends on two factors: 1) the delay for retransmissions, and 2) the delay imposed by the occurrence of busy TSs. Below we first derive the PMF of the end-to-end packet delay incurred purely due to retransmissions, when there are no sensed busy TSs. Then, the delay of the general cases including both sensed busy and free TSs between the first transmission and the final successful reception of a packet is considered.

Firstly, when the sensing results at the CU indicate that there is no busy TS between the first transmission and the final reception of a packet, the probability that n TSs are used for successfully delivering a packet can be expressed as

$$\begin{aligned}
P_{MF}(n) &= \Bigg(\sum_{j=0}^{n-1}\binom{n-1}{j}(P_{on}P_{md})^j(P_{off}(1-P_{fa})\\
&\qquad\cdot P_e)^{n-j-1}(1-P_e)P_A\Bigg), \quad n=1,2,\ldots \qquad (22)
\end{aligned}$$

For explicit clarity, the above equation can be explained as:

- $(P_{on}P_{md})^j$ defines the probability that j out of $(n-1)$ TSs are detected to be free by CU due to mis-detection and thus the transmissions on these TSs are always in error.
- $(P_{off}(1-P_{fa})\cdot P_e)^{n-j-1}$ represents the probability that the remaining $(n-j-1)$ TSs are free and indeed they are detected to be free by the CU and that transmission takes place in these TSs. However, due to channel noise, the packets transmitted in these $(n-j-1)$ TSs are received in error, which results in retransmission.
- Finally, $(1-P_e)P_A$ is the probability that the final TS is free as well as it is correctly sensed, and hence the packet is successfully delivered.

Secondly, in the general cases that there might be busy TSs between the first transmission and the final reception of a packet, the probability that n TSs are used can be expressed as

$$\begin{aligned}
P_{MF}(n) &= \sum_{i=0}^{n-2}\sum_{j=0}^{n-i-1}\binom{n-2}{i}\binom{n-i-1}{j}(P_{bs})^i\\
&\quad\cdot(P_{on}P_{md})^j(P_{off}(1-P_{fa})P_e)^{n-i-j-1}\\
&\quad\cdot(1-P_e)P_A, \quad n=1,2,\ldots \qquad (23)
\end{aligned}$$

where, in addition to the terms that are similar to those in (22), $\binom{n-2}{i}P_{bs}^i$ represents the probability that there are i sensed busy TSs between the first transmission and the final reception of a packet. Note that the largest value for i is $n-2$, as the first and the last TSs are sensed to be free.

2) AVERAGE END-TO-END PACKET DELAY

Having obtained the PMF of the end-to-end packet delay, which is given by Eq. (23), the average end-to-end packet delay quantified in terms of TSs can be expressed as

$$\begin{aligned}
\tau &= \sum_{n=1}^{\infty} n\cdot P_{MF}(n)\\
&\approx \sum_{n=1}^{M_T} n\cdot P_{MF}(n), \text{ (TSs)} \qquad (24)
\end{aligned}$$

where M_T is set as the maximum delay to be considered. Note that M_T can be rendered of ensuring that the unconsidered components becomes negligible. For example, we may choose M_T to satisfy $\sum_{m=1}^{M_T} P_{MF}(m) = 1-10^{-8}$.

C. THROUGHPUT

Given the average packet delay expression of (20), we can readily obtain the throughput of the CU system operated under the CSW-HARQ, which can be expressed as

$$\begin{aligned}
R_s &= \frac{1}{T_D}\\
&= \frac{N}{T}\left(\frac{(P_B+P_AP_e-1)^2}{P_A(1-P_e)(1+N_{DP})}\right)\text{ (PPS)} \qquad (25)\\
&= N\left(\frac{(P_B+P_AP_e-1)^2}{P_A(1-P_e)(1+N_{DP})}\right)\text{ (PPTS)} \qquad (26)\\
&= \frac{N}{k+N}\left(\frac{(P_B+P_AP_e-1)^2}{P_A(1-P_e)(1+N_{DP})}\right)\text{ (PPT}_p\text{)}, \qquad (27)
\end{aligned}$$

where PPS, PPTS and PPT$_p$ denote packet per second, packet per TS and packet per T_p, respectively. Furthermore, let us assume that a (N_D, K_d) RS code is employed denote by B the

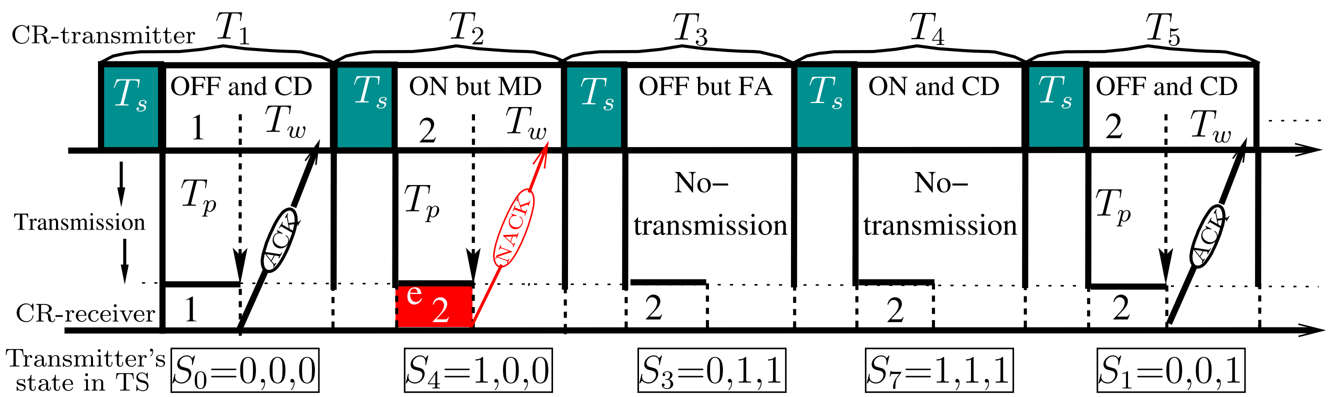

FIGURE 11. Transmission flow of CSW-HARQ, where CD, MD and FA are for correct-detection, mis-detection and false-alarm, respectively. The state is observed by the transmitter at the end of TS.

number of bits per code symbol. Then, the throughput can also be expressed in terms of bits per second (bps) as

$$R_s = \frac{1}{T_D} \cdot K_d \cdot B \text{ (bps)}. \tag{28}$$

Above we have analyzed the performance of the proposed CSW-HARQ scheme using the probability-based approach. In the following section, we also provide a Markov-chain based approach for analysing the CSW-HARQ scheme.

V. MARKOV CHAIN-BASED ANALYSIS OF THE CSW-HARQ SCHEME

In this section, we first model the CSW-HARQ scheme relying on realistic imperfect sensing using the DTMC. Then, we analyze the stationary throughput of the CSW-HARQ. Finally, we analyse the end-to-end packet delay by conceiving both its PMF and the average end-to-end packet delay.

Let us first define the states of the CSW-HARQ, where a state can be jointly defined by 1) the real status of the PU's channel (μ), 2) the status of the PU's channel sensed by the CU (ν), and 3) the status of a specific packet (ξ), which is either a new or an old packet stored in the transmitter's buffer. The state is observed and updated at the end of each TS. Let us express the eight legitimate states as

$$\mathbb{S} = \{S_0, S_1, S_2, \ldots, S_7\}, \tag{29}$$

where each state is a binary number of length 3, expressed as

$$S_i = \{\mu, \nu, \xi\}, \tag{30}$$

where the index i represents the decimal value given by $\{\mu\nu\xi\}$. In (30), μ, ν and ξ are defined as

$$\mu = \begin{cases} 0, & \text{the PU's channel is free,} \\ 1, & \text{the PU's channel is busy;} \end{cases} \tag{31}$$

$$\nu = \begin{cases} 0, & \text{the PU's channel is sensed to be free,} \\ 1, & \text{the PU's channel is sensed to be busy;} \end{cases} \tag{32}$$

and

$$\xi = \begin{cases} 0, & \text{if the packet stored in the transmitter} \\ & \text{buffer is a new packet,} \\ 1, & \text{if the packet stored in the transmitter} \\ & \text{buffer is an old packet.} \end{cases} \tag{33}$$

As an example, Fig. 11 illustrates the transitions between states in the context of five TSs. The number in the boxes of the CU transmitter and the receiver represents the packet that is transmitted and received, respectively. In more detail, Fig. 11 is interpreted as follows.

(a) Assume that during TS T_1, the PU's channel is free and it is correctly sensed to be free corresponding to $\mu = 0$, $\nu = 0$. Assume furthermore that a new packet which gives $\xi = 0$ is transmitted. Hence, the state observed by transmitter in this TS is $S_0 = \{0, 0, 0\}$. As shown in the figure, we assume that the packet is correctly received and hence an ACK flag is sent by the receiver to the transmitter as seen in Fig. 11.

(b) As a benefit of the error-free transmission in the TS T_1, the transmitter buffer is updated to a new packet. In TS T_2, the PU's channel is busy, but it is mis-detected by the CU transmitter. Therefore, a new packet waiting in the buffer is transmitted in TS T_2. Hence, the state during TS T_2 is $S_4 = \{1, 0, 0\}$. Furthermore, it can be shown that the transition from S_0 to S_4 takes place with a probability of $P_{0,4} = (1 - P_e)P_{on}P_{md}$. Note that, due to the mis-detection of the busy PU's channel, the packet sent in TS T_2 is received in error and hence, a NACK flag is fed back.

(c) Still referencing to Fig. 11 in TS T_3, the PU channel is free but it is found busy due to false-alarm. Since the transmission in TS T_2 is erroneous and the packet requires retransmission, hence the state of the transmitter in TS T_3 is $S_3 = \{0, 1, 1\}$ with the transition probability $P_{4,3} = P_{off}P_{fa}$.

(d) Similarly, we can find that the state during TS T_4 is $S_7 = \{1, 1, 1\}$. The transition from S_3 to S_7 takes place with a probability of $P_{3,7} = P_{on}(1 - P_{md})$.

(e) Finally, in TS T_5, the PU's channel is correctly detected to be free and therefore the old packet stored in the transmitter buffer is transmitted, which results in the transition from state S_7 to S_1 in Fig. 11, with the transition probability of $P_{7,1} = P_{off}(1 - P_{fa})$.

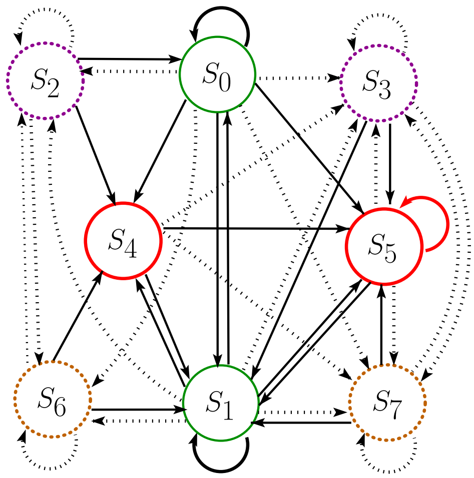

FIGURE 12. The state transition diagram for the DTMC modelling the proposed CSW-HARQ scheme, where *dashed* lines correspond to the transitions towards busy states, while *solid* lines illustrate the transitions towards free states. The *solid green* and *red* circles represent the states in which the PU's channel is free due to correct detection and mis-detection, respectively, while *dashed brown* and *magenta* color circles represent the state in which the PU's channel is found busy due to correct detection and false-alarm, respectively.

Following the above analysis, we can see that the legitimate state to state transitions can be summarized, as shown in Fig. 12. Let the state-transition matrix be expressed as $\mathbf{P}$, where the (i, j)th element of has the transition probability $P_{i,j}$, which can be found as shown in the above example. Furthermore, according to the properties of the DTMC [14], [83], we have

$$0 \leq P_{i,j} \leq 1.$$

$$\sum_{j=0}^{7} P_{i,j} = 1, \quad \forall S_i \in \mathbb{S}, \tag{34}$$

In TS (n), the transmitter is in one of the eight legitimate states with the probability of $\boldsymbol{p}(n) = [P_0(n), P_1(n), \ldots, P_7(n)]^T$. Then, in TS $(n+1)$, the probabilities of the eight possible states can be found from [14], [84]

$$\boldsymbol{p}(n+1) = \mathbf{P}^T \boldsymbol{p}(n). \tag{35}$$

According to [84], when $n \to \infty$, the Markov chain reaches its steady-state condition [14], and in this case we have

$$\boldsymbol{p}(n+1) = \boldsymbol{p}(n). \tag{36}$$

Let the steady-state probabilities be expressed as $\boldsymbol{\pi} = \lim_{n\to\infty} \boldsymbol{p}(n)$, where we have $\boldsymbol{\pi} = [\pi_0, \pi_2 \ldots, \pi_i \ldots]^T$, and π_i represents the steady state probability that the transmitter is in state S_i. Then, from (35) and (36) we have

$$\boldsymbol{\pi} = \mathbf{P}^T \boldsymbol{\pi}, \tag{37}$$

which shows that the steady state probabilities of the different states which can be obtained by computing the right eigenvector of $\mathbf{P}^T$ corresponding to the eigenvalue of 1 [14], [83], [84]. Note that the steady state probabilities satisfy the relationship of

$$\sum_{j\in\mathbb{S}} \pi_j = 1 \text{ or } \boldsymbol{\pi}^T \times \mathbf{1} = 1, \tag{38}$$

where $\mathbf{1}$ represents a unit of column vector.

A. THROUGHPUT OF CSW-HARQ

As defined in Section IV, the throughput of the CSW-HARQ scheme is the rate of successful transmission per TS. Carrying out a successful transmission depends on two factors: 1) a free TS is successfully sensed, and 2) error-free transmission is a achieved. Hence, as shown in (37), when the DTMC reaches its steady state, the throughput of the CSW-HARQ scheme can be obtained from specific state transitions yielding a successful transmission. According to the definition of states in (30) and Fig. 12, the transmission of new packet is only possible when the CU transmitter is in state S_0 or S_4. Therefore, the achievable throughput of the CSW-HARQ is given by

$$R_s = \pi_0 + \pi_4 \text{ (packets / TS)}. \tag{39}$$

Additionally, using $T = (T_d + T_s)T_p$, the throughput quantified in terms of the number of packets per T_p can be expressed as

$$R'_s = \frac{1}{T} \cdot R_s \text{ (packets / } T_p). \tag{40}$$

Let us now analyze the delay of the CSW-HARQ scheme under the DTMC framework.

B. DELAY ANALYSIS OF CSW-HARQ

In this subsection, we analyse both the average packet delay and the end-to-end packet delay with the aid of the DTMC model of the CSW-HARQ. For the end-to-end packet delay, we derive both its probability distribution and the average end-to-end packet delay.

1) AVERAGE PACKET DELAY (T_D)

The average packet delay is defined as the average number of TSs or T_p's needed for the successful transmission of a packet. After obtaining the achievable throughput of Eqs. (39) or (40), the average packet delay can be readily obtained, which can be expressed as

$$T_D = \frac{1}{R_s} \text{ (TS per packet)} \tag{41}$$

$$= \frac{k+N}{R_s} \text{ (} T_p\text{'s per packet).} \tag{42}$$

2) END-TO-END PACKET DELAY

We first analyze the probability distribution of the end-to-end packet delay. Let $\mathbb{S}_N$ be the specific subset of $\mathbb{S}$, which contains the subsets of states $\mathbb{S}_i$. Here, $\mathbb{S}_i$ is a subset that a new packet transmitted from state S_i is correctly received in state S_j, with the delay of m TSs, i.e.,

$$\mathbb{S}_i = \{S_j| \text{ a new packet transmitted from } S_i \text{ is correctly received in state } S_j \text{ after a a delay of } m \text{ TSs}\}, \tag{43}$$

where we have $\mathbb{S}_i \subset \mathbb{S}_N$. Following the above definitions, the probability mass function of the end-to-end packet delay can be formulated as

$$P(m) = \frac{1}{(\pi_0 + \pi_4)} \sum_{S_i \in \mathbb{S}_N} \sum_{S_j \in \mathbb{S}} \pi_i \cdot P^{(m)}_{i,j}, \quad m = 1, 2 \ldots \tag{44}$$

$$= \frac{\pi_0}{\pi_0 + \pi_4} \sum_{S_j \in \mathbb{S}_0} P^{(m)}_{0,j} + \frac{\pi_4}{\pi_0 + \pi_4} \sum_{S_j \in \mathbb{S}_4} P^{(m)}_{4,j}, \tag{45}$$

where $P^{(m)}_{i,j}$ denotes the transition probability from state S_i to state S_j after a delay of m TSs.

Let us express the PMF of the end-to-end packet delay as

$$\boldsymbol{P}_{MF} = [P(1), P(2), \ldots, P(M_T)]^T, \tag{46}$$

where M_T is the largest delay considered, beyond which the probability of occurrence becomes negligible. From the properties of the DTMC, we know that given a state S_i, after q transitions, we have

$$\boldsymbol{p}^{(q)} = (\mathbf{P}^T)^q \boldsymbol{e}_i, \; q = 1, 2, \ldots \tag{47}$$

where $\boldsymbol{e}_i$ is the ith column of the identity matrix. From (47) we can see that whenever we multiply $\mathbf{P}^T$ on a current $\boldsymbol{p}^q$, we can obtain the following information:

a) The end-to-end packet delay is q TSs, if the packet is firstly transmitted in state S_i is correctly received in some states after q TSs.
b) The transition probabilities from state S_i to any of the states in $\mathbb{S}$, which contains the states generating the end-to-end delay of q TSs.
c) The transition probabilities from state S_i to any other states without resulting in correct reception of the packet firstly sent in state S_i.

Using the above information, we can update $\boldsymbol{P}_{MF}$ by the following formula.

$$P(m) \leftarrow P(m) + \pi_i \cdot P^{(m)}_{i,j}, \quad m = 1, 2 \ldots, M_T, \quad S_j \in \mathbb{S}, \; S_i \in \mathbb{S}_N. \tag{48}$$

Finally, when $\boldsymbol{P}_{MF}$ does not change, we can compute the average end-to-end packet delay, which can be formulated as

$$\tau = \sum_{i=1}^{M_T} i \cdot P(i) \text{ (TSs)} \tag{49}$$

$$= \sum_{i=1}^{M} i(k + N)P(i)T'_p s. \tag{50}$$

After completion of our theoretical analysis of the proposed CSW-HARQ scheme, we proceed to validate the accuracy of both the approaches discussed in Sections IV and V by comparing the analytical results to those obtained through simulations.

VI. PERFORMANCE RESULTS

In this section, we demonstrate the performance of the CSW-HARQ system in terms of three performance metrics, namely, 1) throughput 2) average packet delay and 3) end-to-end packet delay, when both idealized perfect sensing and practical imperfect sensing environments are considered. We will characterize the impact of the false-alarm probability (P_{fa}), of the mis-detection probability (P_{md}), the channel's busy probability (P_{on}) and of the packet error probability (P_e) on the performance. Note that, in the case of perfect sensing, P_{fa} and P_{md} are always zero. In our studies, Matlab-based simulations are used, and fifty thousand packets are transmitted for every specific conditions. The observation period commences from the first TS, which continues until all packets are successfully received by the CU receiver.

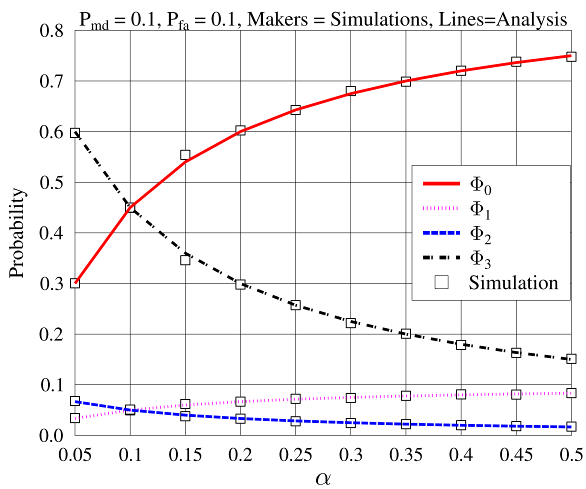

FIGURE 13. Steady-state probabilities of $[\Phi_0, \Phi_1, \Phi_2, \Phi_3]$ seen in (9) with respect to α.

Fig. 13 shows the correct detection probability Φ_0 of a free channel, the false-alarm probability Φ_1, the mis-detection probability Φ_2 and the correct detection probability Φ_3 of a busy channel, as seen in (9) of Section II-B, with respect to the parameter α. It can be seen from Fig. 13 that when the transmission chances for a CU over those of a PU channel increase, i.e., when α increases, $P_{off} = \Phi_0$ also significantly increases, while $P_{fa} = \Phi_1$ increases only slightly. The slight increase in P_{fa} is the consequence of imperfect sensing. On the other hand, when α increases, P_{on} is dramatically reduced, while P_{md} exhibits only a moderate reduction. As shown in Fig. 13, the analytical results evaluated from Eq. (9) closely agree with the simulation results.

Fig. 14 depicts the throughput achieved by the CSW-HARQ scheme both for perfect and imperfect sensing versus the packet error probability P_e and with respect to the

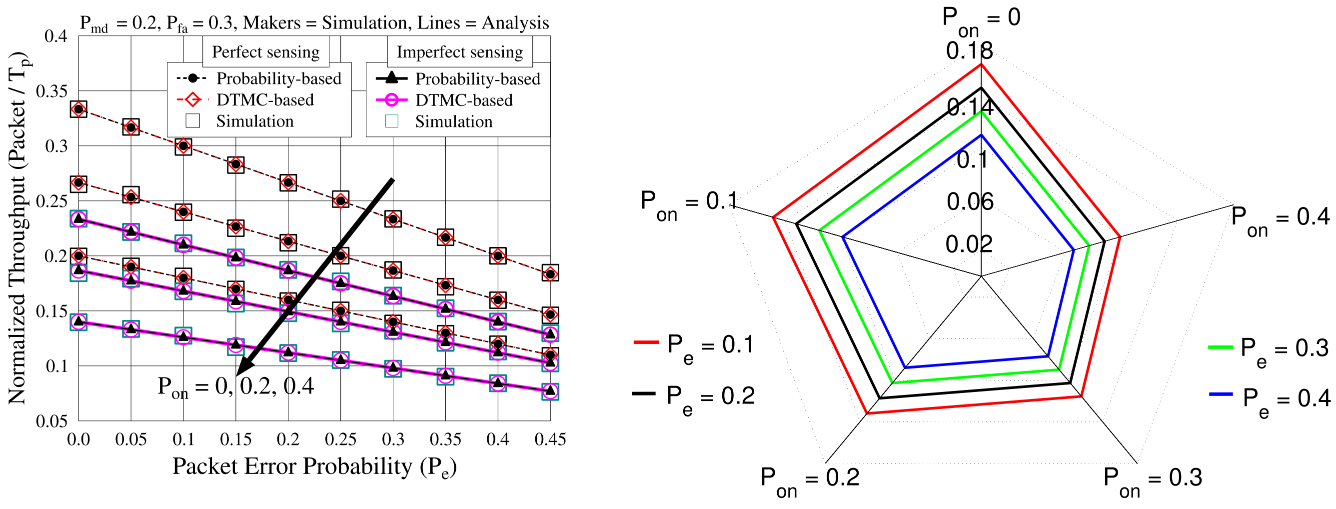

(a) (b)

FIGURE 14. Normalized Throughput in terms of T_p versus packet error probability P_e for the CSW-HARQ scheme associated with various channel busy probabilities P_{on}, when assuming $T_s = 1T_p$ and $T_d = 2T_p$. a) Throughput is investigated in both perfect and imperfect cases, where in the case of imperfect sensing $P_{md} = 0.3$ and $P_{fa} = 0.2$. b) Throughput is again analyzed in realistic imperfect sensing, when $P_{md} = 0.45$ and $P_{fa} = 0.45$ for different values of P_e and P_{on}.

probability P_{on} of the channel being busy. In our simulations, the throughput is calculated as

$$R'_S = \frac{N_s}{N_t} \cdot \frac{T_p}{T_s + T_d} \text{ (packets per } T_p), \tag{51}$$

where N_t represents the total number of TSs used for the successful transmission of N_s packets by the CU.

As shown in Fig. 14, the throughput is at its maximum, when the channel is perfectly reliable, i.e. when $P_e = 0$ for both the perfect and imperfect sensing scenarios. As P_e increases, implying that the channel becomes less reliable, the achievable throughput reduces nearly linearly with P_e, which is a direct consequence of retransmissions. At a given P_e, the throughput attains its maximum, when the channel is always free to use, i.e. when $P_{on} = 0$. However, as P_{on} increases, the attainable throughput significantly reducing, since the CU has to wait longer for finding free channels for its data transmission. Furthermore, Fig. 14 shows that realistic imperfect sensing may result in a significant throughout drop, implying that indeed it is important to achieve reliable sensing in cognitive radios.

Additionally, Fig. 14(a) shows that the analytical results evaluated from Eqs. (27) and (40) agree well with the simulation results.

Having characterized the throughput, let us now elaborate on the delay of the CSW-HARQ scheme. Firstly, we consider the average packet delay, as shown in Fig. 15. Note that for the results obtained by simulations, the average packet delay is given by the total number of TSs N_T used for the successful transmission of N_s packets, divided by N_s, which is expressed as

$$T_{DS} = \frac{N_t \cdot (T_s + T_d)}{N_s} \text{ (seconds)}. \tag{52}$$

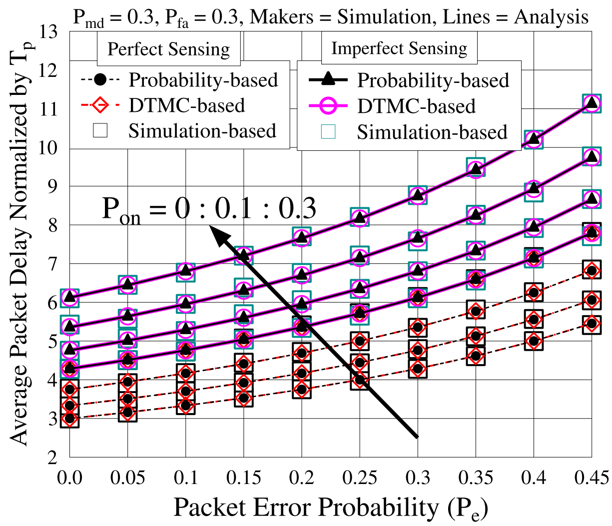

FIGURE 15. Average packet delay of the CSW-HARQ system versus P_e for various channel busy probabilities when either perfect sensing ($P_{fa} = P_{md} = 0$) or imperfect sensing ($P_{fa} = P_{md} = 0.3$) are considered.

The results depicted in Fig. 15 are normalized by T_p, yielding:

$$T'_{DS} = \frac{T_{DS}}{T_p} \ (T_p s). \tag{53}$$

In Fig. 15, the average packet delay of the CSW-HARQ system is studied, both for perfect and imperfect sensing. For a given P_{on}, the average packet delay is at its minimum, when P_e is zero and it increases, when P_e or/and P_{on} increases. As discussed above, the increase of P_e triggers more retransmissions, while the increase of P_{on} reduces the transmission opportunities for the CU's, which hence result in the increase of the average packet delay.

Additionally, imperfect sensing results in the mis-use of the channel, which increases the average delay. Finally, as shown in Fig. 15, the results obtained both from our probability-based and from the DTMC-based approaches are accurate, closely agreeing with on simulation results.

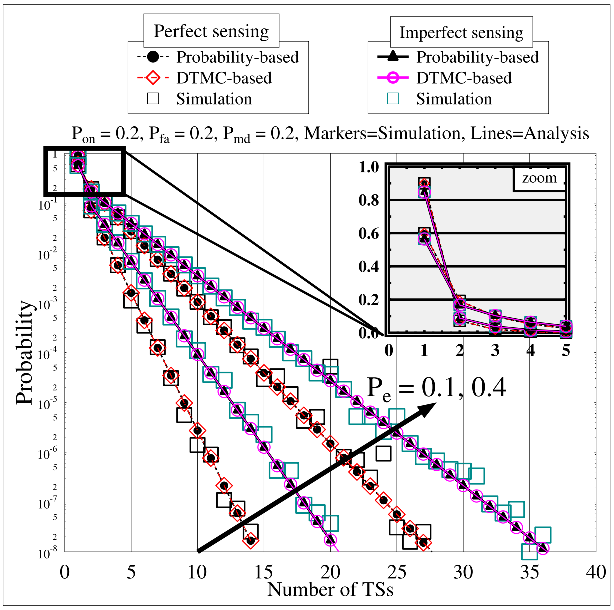

FIGURE 16. Probability of the end-to-end packet delay in the perfect ($P_{fa} = P_{md} = 0$) and imperfect ($P_{fa} = P_{md} = 0.2$) sensing scenarios for $P_{on} = 0.2$ and $P_e = \{0.1, 0.4\}$.

In Fig. 16, we depict the end-to-end packet delay of the CSW-HARQ scheme in terms of both perfect and imperfect sensing. In the simulations, the end-to-end delay is evaluated as the total time duration from each individual packet's first transmission until its successful reception, divided by the total number of packets, N_s. In detail, let a vector $\boldsymbol{d}$ of length N_s be used to store the end-to-end delay experienced by each of the N_s transmitted packets. Specifically, $\boldsymbol{d}(j)$ represents the end-to-end delay of the jth packet. Then, the PMF of the end-to-end packet delay illustrated in Fig. 16 is given by

$$\boldsymbol{P}_d(i) = \frac{\sum_{j=1}^{N_s} \delta\left(d(j) - i\right)}{N_s}, \quad 1 \leq i \leq \max(\boldsymbol{d}). \tag{54}$$

Observe from Fig. 16 that in the case of perfect sensing, 90% of the packets are successfully received with an end-to-end delay of one TS, when $P_e = 0.1$, as accurately shown in the zoomed-in portion of the figure. To elaborate further, Following is 7.2% of packets are correctly received with an end-to-end delay of 2 TSs, and 2% of the packets are correctly received with an end-to-end delay of 3 TSs, as shown in Fig. 16. On the other hand, in the case of imperfect sensing, at $P_e = 0.1$, the number of packets having an end-to-end delay of one TS is reduced to 84%, and the number packets having an end-to-end delay of 2 and 3 TSs is increased to 8.8% and 3.7%, respectively. By contrast, when P_e is increased to 0.4, the ratio of the packets having an end-to-end delay of one TS is reduced to 60% and 54% in the perfect and imperfect sensing scenarios, respectively. In a similar manner, the ratio of the packets having an end-to-end delay of two or more TSs also reduces correspondingly. Hence, the tail of the PMF curves increases as P_e increases, implying an increase of the end-to-end packet delay.

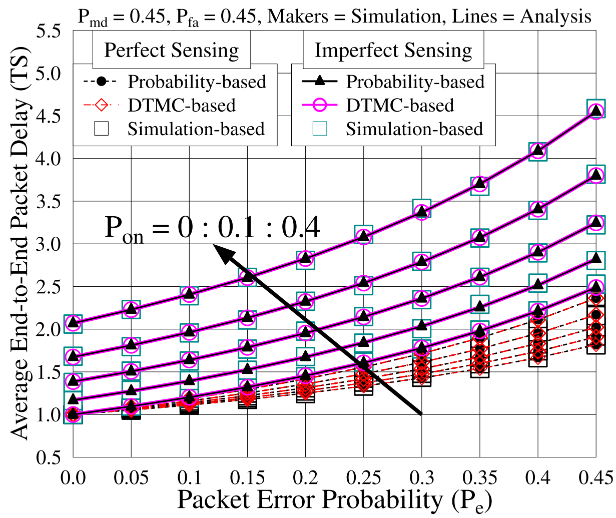

FIGURE 17. Average end-to-end packet delay versus packet error probability (P_e) for the CSW-HARQ with respect to different channel busy probabilities P_{on} and in the case of imperfect sensing.

The average end-to-end packet delay is shown in Fig. 17, where the results gleaned from our simulations are evaluated from the formula

$$\tau_s = \sum_{i=1}^{\max(\boldsymbol{d})} \boldsymbol{P}_d(i) \times i(T) \text{ (seconds)}. \tag{55}$$

It can be observed from Fig. 17 that the average end-to-end packet delay increases, as P_e and/or P_{on} increases. More importantly, it can be seen that in the case of perfect sensing, the average end-to-end packet delay has a minimum of one TS when $P_e = 0$, regardless of the value of P_{on}. This is because, when the channel is highly reliable and when the probability of mis-detection is zero, correct delivery of a transmitted packet is ensured in the first attempt. By contrast, when P_e and/or P_{on} increases, the delay increases significantly, although it remains still lower than the corresponding delay in the case of imperfect sensing. In the case of imperfect sensing, there is a delay caused by the false-alarm and mis-detection of the PU's channel.

Finally, we compare the average packet delay to the average end-to-end packet delay in Fig. 18. Explicitly, for a given scenario, the average packet is always higher than the average end-to-end delay. Furthermore, the average packet delay increases faster than the end-to-end packet delay, when P_e or/and P_{on} increases. This is because, the average packet delay considers all the time spanning from the start of transmitting the first packet until the successful reception of the last packet. By contrast, the end-to-end delay only considers

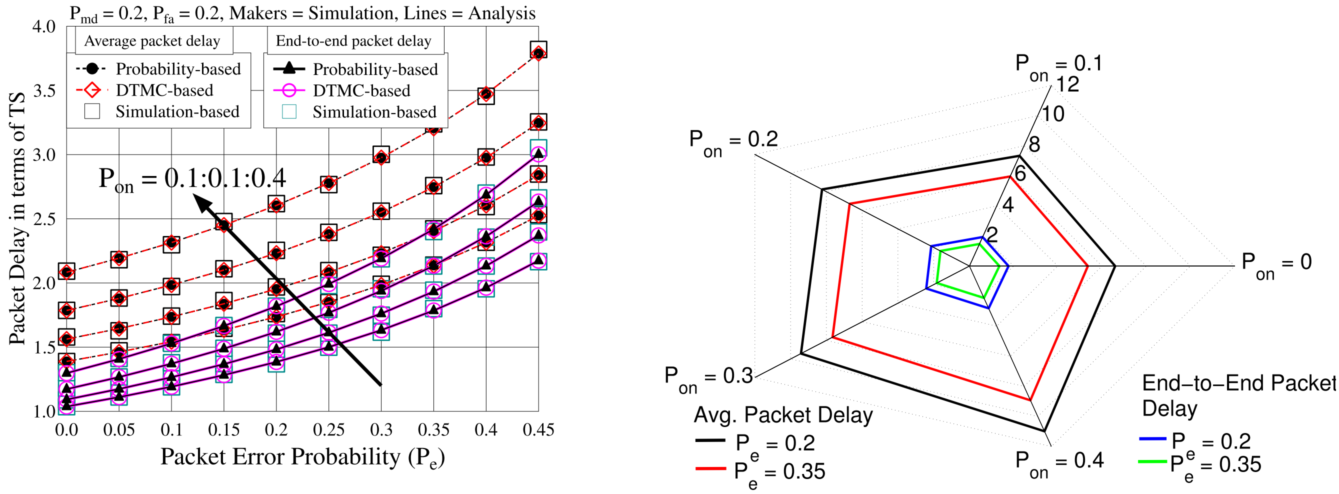

(a) (b)

FIGURE 18. **Comparison of average packet delay and end-to-end packet delay measured in terms of TS, when operating with realistic imperfect sensing. a) Delay versus packet error probability for different values of P_{on}, when $P_{md} = 0.2$ and $P_{fa} = 0.2$. b) Again, both the average packet delay and the end-to-end packet delay are analysed, when $P_{md} = 0.3$ and $P_{fa} = 0.3$.**

TABLE 1. **Performance results summary of the CSW-HARQ scheme in the case of realistic imperfect sensing, when $P_{md} = 0.3$ and $P_{fa} = 0.3$. The results shown are normalized in terms of TS.**

Packet error Probability	P_{on}	Throughput	Average Packet Delay	End-to-end Packet Delay
$P_e = 0$	0	0.233	4.3	1
	0.1	0.210	4.76	1.07
	0.2	0.187	5.35	1.17
	0.3	0.163	6.12	1.31
$P_e = 0.2$	0	0.187	5.35	1.35
	0.1	0.168	5.95	1.47
	0.2	0.149	6.7	1.62
	0.3	0.131	7.65	1.83
$P_e = 0.4$	0	0.14	7.8	1.95
	0.1	0.126	7.94	2.13
	0.2	0.112	8.93	2.36
	0.3	0.098	10.2	2.68

the delay of each individual packet from the instant of its transmission to its correct reception, but it does not consider the time between two successful packets. For more clear insight, we present the performance results in table 1.

VII. CONCLUSIONS

In this paper, we have investigated the performance of the CSW-HARQ transmission scheme both in the perfect and imperfect sensing scenarios. Both the throughput and delay of the CSW-HARQ scheme have been investigated both by analytical and simulation techniques. Furthermore, two analytical approaches, namely the probability-based approach and the DTMC-based approach have been involved for deriving the closed-form formulas of the throughput and delay. Both analytical approaches have been validated by our simulation results. Based on our studies and performance results, we can conclude that the achievable throughput and delay performance of the CSW-HARQ are substantially affected by the activity of the PUs, by the reliability of the CU channels and by the reliability of sensing. When the PU channel becomes busier, the CSW-HARQ's throughput becomes lower and the average packet delay increases, even when the CU sensing and transmission are reliable. When the sensing is reliable, the CSW-HARQ system achieves a higher throughput and a lower delay compared to the cases of imperfect sensing. Given that in CR the opportunity for data transmission is limited, it is vitally important to employ high-reliability sensing approaches for improving the CU's throughput and delay, in addition to minimizing the interference imposed on the PUs.

ACKNOWLEDGMENT

This work has been published in IEEE Vehicular Technology Conference, Glasgow, May 2015.

REFERENCES

[1] A. Goldsmith, S. A. Jafar, I. Maric, and S. Srinivasa, "Breaking spectrum gridlock with cognitive radios: An information theoretic perspective," *Proc. IEEE*, vol. 97, no. 5, pp. 894–914, Apr. 2009.

[2] "Spectrum policy task force," Federal Commun. Commission, Washington, DC, USA, Tech. Rep. ET Docket No. 02-155, Nov. 2002. AQ:3

[3] G. Staple and K. Werbach, "The end of spectrum scarcity [spectrum allocation and utilization]," *IEEE Spectr.*, vol. 41, no. 3, pp. 48–52, Mar. 2004.

[4] M. A. McHenry, P. A. Tenhula, D. McCloskey, D. A. Roberson, and C. S. Hood, "Chicago spectrum occupancy measurements & analysis and a long-term studies proposal," in *Proc. 1st Int. Workshop Technol. Policy Access. Spectr. (TAPAS)*, 2006, Art. no. 1.

[5] J. Yang, "Spatial channel characterization for cognitive radios," M.S. thesis, Dept. EECS, Univ. California, Berkeley, CA, USA, Tech. Rep. UCB/ERL M05/8, Jan. 2005. [Online]. Available: http://www.eecs.berkeley.edu/Pubs/TechRpts/2005/4293.html

[6] D. B. Cabric and R. W. Brodersen, "Cognitive radios: System design perspective," Dept. EECS, Univ. California Berkeley, Berkeley, CA, USA, Tech. Rep. UCB/EECS-2007-156, 2007.

[7] E. Hossain, D. Niyato, and Z. Han, *Dynamic Spectrum Access and Management in Cognitive Radio Networks*. Cambridge, U.K.: Cambridge Univ. Press, 2009.

[8] I. F. Akyildiz, Y. Altunbasak, F. Fekri, and R. Sivakumar, "AdaptNet: An adaptive protocol suite for the next-generation wireless Internet," *IEEE Commun. Mag.*, vol. 42, no. 3, pp. 128–136, Mar. 2004.

[9] Q. Zhao and B. M. Sadler, "A survey of dynamic spectrum access," *IEEE Signal Process. Mag.*, vol. 24, no. 3, pp. 79–89, May 2007.

[10] J. Mitola and G. Q. Maguire, Jr., "Cognitive radio: Making software radios more personal," *IEEE Pers. Commun.*, vol. 6, no. 4, pp. 13–18, Apr. 1999.

[11] S. Haykin, "Cognitive radio: Brain-empowered wireless communications," *IEEE J. Sel. Areas Commun.*, vol. 23, no. 2, pp. 201–220, Feb. 2005.

[12] M. Sherman, A. N. Mody, R. Martinez, C. Rodriguez, and R. Reddy, "IEEE standards supporting cognitive radio and networks, dynamic spectrum access, and coexistence," *IEEE Commun. Mag.*, vol. 46, no. 7, pp. 72–79, Jul. 2008.

[13] S. Chang, "Theory of information feedback systems," *IRE Trans. Inf. Theory*, vol. 2, no. 3, pp. 29–40, Sep. 1956.

[14] D. P. Bertsekas and R. G. Gallager, *Data Networks*, 2nd ed. Englewood Cliffs, NJ, USA: Prentice-Hall, 1991.

[15] S. Lin and D. J. Costello, Jr., *Error Control Coding: Fundamentals and Applications*, 2nd ed. Upper Saddle River, NJ, USA: Prentice-Hall, 1999.

[16] A. Leon-Garcia and I. Widjaja, *Communication Networks*. New York, NY, USA: McGraw-Hill, 2004.

[17] J. W. Wozencraft and M. Horstein, "Digitalised communication over two-way channels," in *Proc. 4th London Symp. Inf. Theory*, London, U.K., Sep. 1960.

[18] J. M. Wozencraft and M. Horstein, "Coding for two-way channels," Res. Lab. Electron., Massachusetts Inst. Technol., Cambridge, MA, USA, Tech. Rep. 383, 1961.

[19] *IEEE Standard for Local and Metropolitan Area Networks Part 16: Air Interface for Fixed and Mobile Broadband Wireless Access Systems Amendment 2: Physical and Medium Access Control Layers for Combined Fixed and Mobile Operation in Licensed Bands and Corrigendum 1*, IEEE Standard 802.16e-2005 and IEEE Standard 802.16-2004/Cor 1-2005 (Amendment and Corrigendum to IEEE Standard 802.16-2004), Feb. 2006, pp. 1–822.

[20] *3rd Generation Partnership Project; Technical Specification Group Radio Access Network; Physical Layer Aspects of UTRA High Speed Downlink Packet Access (Release 4)*, document 3GPP TR 25.848 V4.0.0, 2001.

[21] A. U. Rehman, L. L. Yang, and L. Hanzo, "Performance of cognitive hybrid automatic repeat reQuest: Stop-and-wait," in *Proc. IEEE 81st Veh. Technol. Conf. (VTC Spring)*, May 2015, pp. 1–5.

[22] A. U. Rehman, L. L. Yang, and L. Hanzo, "Performance of cognitive hybrid automatic repeat reQuest: Go-Back-N," in *Proc. IEEE 83rd Veh. Technol. Conf. (VTC Spring)*, May 2016, pp. 1–5.

[23] Y.-C. Liang, Y. Zeng, E. C. Y. Peh, and A. T. Hoang, "Sensing-throughput tradeoff for cognitive radio networks," *IEEE Trans. Wireless Commun.*, vol. 7, no. 4, pp. 1326–1337, Apr. 2008.

[24] H. Su and X. Zhang, "Cross-layer based opportunistic MAC protocols for QoS provisionings over cognitive radio wireless networks," *IEEE J. Sel. Areas Commun.*, vol. 26, no. 1, pp. 118–129, Jan. 2008.

[25] G. Ding *et al.*, "Robust spectrum sensing with crowd sensors," *IEEE Trans. Commun.*, vol. 62, no. 9, pp. 3129–3143, Sep. 2014.

[26] G. Ozcan and M. Gursoy, "Throughput of cognitive radio systems with finite blocklength codes," *IEEE J. Sel. Areas Commun.*, vol. 31, no. 11, pp. 2541–2554, Nov. 2013.

[27] S. Akin and M. C. Gursoy, "Performance analysis of cognitive radio systems under QoS constraints and channel uncertainty," *IEEE Trans. Wireless Commun.*, vol. 10, no. 9, pp. 2883–2895, Sep. 2011.

[28] S. Stotas and A. Nallanathan, "Enhancing the capacity of spectrum sharing cognitive radio networks," *IEEE Trans. Veh. Technol.*, vol. 60, no. 8, pp. 3768–3779, Oct. 2011.

[29] W.-C. Ao and K.-C. Chen, "End-to-end HARQ in cognitive radio networks," in *Proc. IEEE Wireless Commun. Netw. Conf. (WCNC)*, Apr. 2010, pp. 1–6.

[30] C. Lott, O. Milenkovic, and E. Soljanin, "Hybrid ARQ: Theory, state of the art and future directions," in *Proc. IEEE Inf. Theory Workshop Inf. Theory Wireless Netw.*, Jul. 2007, pp. 1–5.

[31] H. O. Burton and D. D. Sullivan, "Errors and error control," *Proc. IEEE*, vol. 60, no. 11, pp. 1293–1301, Nov. 1972.

[32] A. R. K. Sastry, "Improving automatic repeat-request (ARQ) performance on satellite channels under high error rate conditions," *IEEE Trans. Commun.*, vol. 23, no. 4, pp. 436–439, Apr. 1975.

[33] S. Lin, D. J. Costello, and M. J. Miller, "Automatic-repeat-request error-control schemes," *IEEE Commun. Mag.*, vol. 22, no. 12, pp. 5–17, Dec. 1984.

[34] S. Kallel, "Analysis of a type II hybrid ARQ scheme with code combining," *IEEE Trans. Commun.*, vol. 38, no. 8, pp. 1133–1137, Aug. 1990.

[35] L. Hanzo and J. Streit, "Adaptive low-rate wireless videophone schemes," *IEEE Trans. Circuits Syst. Video Technol.*, vol. 5, no. 4, pp. 305–318, Aug. 1995.

[36] M. Zorzi, R. R. Rao, and L. B. Milstein, "ARQ error control for fading mobile radio channels," *IEEE Trans. Veh. Technol.*, vol. 46, no. 2, pp. 445–455, May 1997.

[37] E. M. Sozer, M. Stojanovic, and J. G. Proakis, "Underwater acoustic networks," *IEEE J. Ocean. Eng.*, vol. 25, no. 1, pp. 72–83, Jan. 2000.

[38] Q. Liu, S. Zhou, and G. B. Giannakis, "Cross-layer combining of adaptive modulation and coding with truncated ARQ over wireless links," *IEEE Trans. Wireless Commun.*, vol. 3, no. 5, pp. 1746–1755, Sep. 2004.

[39] J.-F. Cheng, "Coding performance of hybrid ARQ schemes," *IEEE Trans. Commun.*, vol. 54, no. 6, pp. 1017–1029, Jun. 2006.

[40] D. Nguyen, T. Tran, T. Nguyen, and B. Bose, "Wireless broadcast using network coding," *IEEE Trans. Veh. Technol.*, vol. 58, no. 2, pp. 914–925, Feb. 2009.

[41] H. Chen, R. G. Maunder, and L. Hanzo, "Low-complexity multiple-component turbo-decoding-aided hybrid ARQ," *IEEE Trans. Veh. Technol.*, vol. 60, no. 4, pp. 1571–1577, May 2011.

[42] Y. Qin and L.-L. Yang, "Steady-state throughput analysis of network coding nodes employing stop-and-wait automatic repeat request," *IEEE/ACM Trans. Netw.*, vol. 20, no. 5, pp. 1402–1411, Oct. 2012.

[43] B. Zhang, H. Chen, M. El-Hajjar, R. Maunder, and L. Hanzo, "Distributed multiple-component turbo codes for cooperative hybrid ARQ," *IEEE Signal Process. Lett.*, vol. 20, no. 6, pp. 599–602, Jun. 2013.

[44] H. A. Ngo and L. Hanzo, "Hybrid automatic-repeat-reQuest systems for cooperative wireless communications," *IEEE Commun. Surveys Tuts.*, vol. 16, no. 1, pp. 25–45, 1st Quart., 2014.

[45] M. Chitre and W.-S. Soh, "Reliable point-to-point underwater acoustic data transfer: To juggle or not to juggle?" *IEEE J. Ocean. Eng.*, vol. 40, no. 1, pp. 93–103, Jan. 2015.

[46] B. Makki, T. Eriksson, and T. Svensson, "On the performance of the relay–ARQ networks," *IEEE Trans. Veh. Technol.*, vol. 65, no. 4, pp. 2078–2096, Apr. 2016.

[47] I. F. Akyildiz, W.-Y. Lee, M. C. Vuran, and S. Mohanty, "Next generation/dynamic spectrum access/cognitive radio wireless networks: A survey," *Comput. Netw.*, vol. 50, no. 13, pp. 2127–2159, 2006.

[48] A. He *et al.*, "Development of a case-based reasoning cognitive engine for IEEE 802.22 WRAN applications," *ACM SIGMOBILE Mobile Comput. Commun. Rev.*, vol. 13, no. 2, pp. 37–48, 2009.

[49] T. Yucek and H. Arslan, "A survey of spectrum sensing algorithms for cognitive radio applications," *IEEE Commun. Surveys Tuts.*, vol. 11, no. 1, pp. 116–130, First Quarter 2009.

[50] G. Ganesan and Y. Li, "Cooperative spectrum sensing in cognitive radio, part I: Two user networks," *IEEE Trans. Wireless Commun.*, vol. 6, no. 6, pp. 2204–2213, Jun. 2007.

[51] W. Tang, M. Z. Shakir, M. A. Imran, R. Tafazolli, and M. S. Alouini, "Throughput analysis for cognitive radio networks with multiple primary users and imperfect spectrum sensing," *IET Commun.*, vol. 6, no. 17, pp. 2787–2795, Nov. 2012.

[52] L. Hanzo, T. H. Liew, and B. L. Yeap, *Turbo Coding, Turbo Equalisation and Space-Time Coding: For Transmission Over Fading Channels*, 2nd ed. New York, NY, USA: Wiley, 2011.

[53] H. Jianhua, K. R. Subramanian, Y. Zongkai, and C. Wenqing, "Analysis of a new broadcast protocol for satellite communications," *IEEE Commun. Lett.*, vol. 4, no. 12, pp. 423–425, Dec. 2000.

[54] P. A. Chou, A. E. Mohr, A. Wang, and S. Mehrotra, "Error control for receiver-driven layered multicast of audio and video," *IEEE Trans. Multimedia*, vol. 3, no. 1, pp. 108–122, Mar. 2001.

[55] B. Zhao and M. C. Valenti, "Practical relay networks: A generalization of hybrid-ARQ," *IEEE J. Sel. Areas Commun.*, vol. 23, no. 1, pp. 7–18, Jan. 2005.

[56] R. Zhang and L. Hanzo, "Superposition-aided delay-constrained hybrid automatic repeat reQuest," *IEEE Trans. Veh. Technol.*, vol. 59, no. 4, pp. 2109–2115, May 2010.

[57] H. Chen, R. G. Maunder, and L. Hanzo, "Lookup-table-based deferred-iteration aided low-complexity turbo hybrid ARQ," *IEEE Trans. Veh. Technol.*, vol. 60, no. 7, pp. 3045–3053, Sep. 2011.

[58] H. Chen, R. G. Maunder, and L. Hanzo, "Deferred-iteration aided low-complexity turbo hybrid ARQ relying on a look-up table," in *Proc. IEEE Global Telecommun. Conf. (GLOBECOM)*, Dec. 2011, pp. 1–5.

[59] S. De, A. Sharma, R. Jantti, and D. H. Cavdar, "Channel adaptive stop-and-wait automatic repeat request protocols for short-range wireless links," *IET Commun.*, vol. 6, no. 14, pp. 2128–2137, Sep. 2012.

[60] *IEEE Standard for Local and Metropolitan Area Networks—Part 20: Air Interface for Mobile Broadband Wireless Access Systems Supporting Vehicular Mobility—Physical and Media Access Control Layer Specification*, IEEE Standard 802.20-2008, Aug. 2008, pp. 1–1039.

[61] *IEEE Standard for Local and Metropolitan Area Networks Part 16: Air Interface for Broadband Wireless Access Systems*, IEEE Standard 802.16m-2011 (Amendment to IEEE Standard 802.16-2009), May 2011, pp. 1–1112.

[62] *IEEE Standard for WirelessMAN-Advanced Air Interface for Broadband Wireless Access Systems*, IEEE Standard 802.16.1-2012, Sep. 2012, pp. 1–1090.

[63] J. Neel, R. M. Buehrer, B. H. Reed, and R. P. Gilles, "Game theoretic analysis of a network of cognitive radios," in *Proc. 45th Midwest Symp. Circuits Syst. (MWSCAS)*, vol. 3. Aug. 2002, pp. III-409–III-412.

[64] *IEEE 802.22 Working Group on Wireless Regional Area Networks Enabling Broadband Wireless Access Using Cognitive Radio Technology and Spectrum Sharing in White Spaces*, IEEE Standard 802.22-2005, 2005.

[65] H. Kushwaha, Y. Xing, R. Chandramouli, and H. Heffes, "Reliable multimedia transmission over cognitive radio networks using fountain codes," *Proc. IEEE*, vol. 96, no. 1, pp. 155–165, Jan. 2008.

[66] S.-Y. Jeon and D.-H. Cho, "An ARQ mechanism considering resource and traffic priorities in cognitive radio systems," *IEEE Commun. Lett.*, vol. 13, no. 7, pp. 504–506, Jul. 2009.

[67] Y.-C. Liang, K.-C. Chen, G. Y. Li, and P. Mahonen, "Cognitive radio networking and communications: An overview," *IEEE Trans. Veh. Technol.*, vol. 60, no. 7, pp. 3386–3407, Sep. 2011.

[68] Y. Yang, H. Ma, and S. Aissa, "Cross-layer combining of adaptive modulation and truncated ARQ under cognitive radio resource requirements," *IEEE Trans. Veh. Technol.*, vol. 61, no. 9, pp. 4020–4030, Nov. 2012.

[69] J. C. F. Li, W. Zhang, A. Nosratinia, and J. Yuan, "SHARP: Spectrum harvesting with ARQ retransmission and probing in cognitive radio," *IEEE Trans. Commun.*, vol. 61, no. 3, pp. 951–960, Mar. 2013.

[70] D. Hamza and S. Aissa, "Enhanced primary and secondary performance through cognitive relaying and leveraging primary feedback," *IEEE Trans. Veh. Technol.*, vol. 63, no. 5, pp. 2236–2247, Jun. 2014.

[71] J. S. Harsini and M. Zorzi, "Transmission strategy design in cognitive radio systems with primary ARQ control and QoS provisioning," *IEEE Trans. Commun.*, vol. 62, no. 6, pp. 1790–1802, Jun. 2014.

[72] S. Touati, H. Boujemaa, and N. Abed, "Cooperative ARQ protocols for underlay cognitive radio networks," in *Proc. 21st Eur. Signal Process. Conf. (EUSIPCO)*, Sep. 2013, pp. 1–5.

[73] G. Yue, X. Wang, and M. Madihian, "Design of anti-jamming coding for cognitive radio," in *Proc. IEEE Global Telecommun. Conf.*, Nov. 2007, pp. 4190–4194.

[74] G. Yue and X. Wang, "Design of efficient ARQ schemes with anti-jamming coding for cognitive radios," in *Proc. IEEE Wireless Commun. Netw. Conf. (WCNC)*, Apr. 2009, pp. 1–6.

[75] Y. Liu, Z. Feng, and P. Zhang, "A novel ARQ scheme based on network coding theory in cognitive radio networks," in *Proc. IEEE Int. Conf. Wireless Inf. Technol. Syst. (ICWITS)*, Aug./Sep. 2010, pp. 1–4.

[76] B. Makki, A. G. I. Amat, and T. Eriksson, "HARQ feedback in spectrum sharing networks," *IEEE Commun. Lett.*, vol. 16, no. 9, pp. 1337–1340, Sep. 2012.

[77] B. Makki, T. Svensson, and M. Zorzi, "Finite block-length analysis of spectrum sharing networks using rate adaptation," *IEEE Trans. Commun.*, vol. 63, no. 8, pp. 2823–2835, Aug. 2015.

[78] W. Liang, S. X. Ng, J. Feng, and L. Hanzo, "Pragmatic distributed algorithm for spectral access in cooperative cognitive radio networks," *IEEE Trans. Commun.*, vol. 62, no. 4, pp. 1188–1200, Apr. 2014.

[79] J. Hu, L. L. Yang, and L. Hanzo, "Maximum average service rate and optimal queue scheduling of delay-constrained hybrid cognitive radio in Nakagami fading channels," *IEEE Trans. Veh. Technol.*, vol. 62, no. 5, pp. 2220–2229, Jun. 2013.

[80] C. Cormio and K. R. Chowdhury, "A survey on MAC protocols for cognitive radio networks," *Ad Hoc Netw.*, vol. 7, no. 7, pp. 1315–1329, Sep. 2009.

[81] A. De Domenico, E. Strinati, and M.-G. Di Benedetto, "A survey on MAC strategies for cognitive radio networks," *IEEE Commun. Surveys Tuts.*, vol. 14, no. 1, pp. 21–44, 1st Quart., 2012.

[82] S. Agarwal and S. De, "eDSA: Energy-efficient dynamic spectrum access protocols for cognitive radio networks," *IEEE Trans. Mobile Comput.*, to be published. AQ:5

[83] R. A. Howard, *Dynamic Probabilistic Systems: Markov Models*. New York, NY, USA: Wiley, 1971.

[84] R. A. Horn and C. R. Johnson, *Matrix Analysis*. Cambridge, U.K.: Cambridge Univ. Press, 2012.

ATEEQ UR REHMAN received the B.Eng. degree in computer science and information technology from the Islamic University of Technology, Dhaka, Bangladesh, in 2009. He is currently pursuing the Ph.D. degree in wireless communications with the University of Southampton under the supervision of Prof L.-L Yang and Prof L. Hanzo. He joined the Department of Computer Science, Abdul Wali Khan University Mardan, Pakistan, as a Lecturer. His main research interests are next generation wireless communications and cognitive radio networks, particularly cross layer approach, and hybrid ARQ.

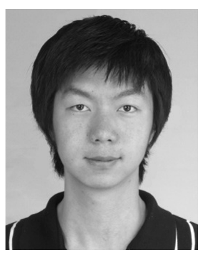

CHEN DONG received the B.S. degree in electronic information sciences and technology from the University of Science and Technology of China, Hefei, China, in 2004, and the M.Eng. degree in pattern recognition and automatic equipment from the University of Chinese Academy of Sciences, Beijing, China, in 2007, and the Ph.D. degree from the University of Southampton, U.K., in 2014. He holds a post-doctoral position with the University of Southampton. He was a recipient of Scholarship under the U.K.-China Scholarships for Excellence programme and he received the best paper award at the IEEE VTC 2014-Fall. His research interests include applied math, relay system, channel modelling, and cross-layer optimization.

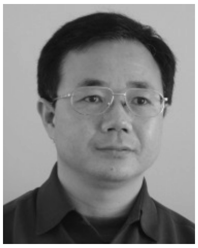

LIE-LIANG YANG (M'98–SM'02) received the B.Eng. degree in communications engineering from Shanghai TieDao University, Shanghai, China, in 1988, and the M.Eng. and Ph.D. degrees in communications and electronics from Northern (Beijing) Jiaotong University, Beijing, China, in 1991 and 1997, respectively. In 1997, he was a Visiting Scientist with the Institute of Radio Engineering and Electronics, Academy of Sciences of the Czech Republic. Since 1997, he has been with the University of Southampton, U.K., where he is currently a Professor of Wireless Communications with the School of Electronics and Computer Science. He has authored over 300 research papers in journals and conference proceedings, authored/co-authored three books and also published several book chapters. His research has covered a wide range of topics in wireless communications, networking and signal processing. He is a fellow of the IET, served as an Associate Editor to the IEEE Transactions on Vehicular Technology and the *Journal of Communications and Networks*, and he is currently an Associate Editor of the IEEE Access and the *Security and Communication Networks Journal*.

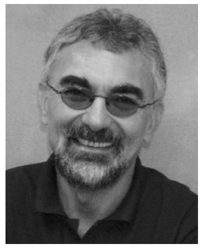

LAJOS HANZO received the D.Sc. degree in electronics in 1976 and the Ph.D. degree in 1983. During his 40-year career in telecommunications he has held various research and academic posts in Hungary, Germany, and the U.K. Since 1986, he has been with the School of Electronics and Computer Science, University of Southampton, U.K., where he holds the chair in telecommunications. He has successfully supervised 110 Ph.D. students. He has co-authored over a 20 John Wiley/IEEE Press books on mobile radio communications totalling in excess of 10 000 pages, published 1595 research contributions at the IEEE Xplore, where he was a TPC and General Chair of IEEE conferences, presented keynote lectures and has been awarded a number of distinctions. He is currently directing a 60-strong academic research team, where he is involved in a range of research projects in the field of wireless multimedia communications sponsored by industry, the Engineering and Physical Sciences Research Council, U.K., the European IST Programme and the Mobile Virtual Centre of Excellence, U.K. He is an Enthusiastic Supporter of industrial and academic liaison and he offers a range of industrial courses. He is also a Governor of the IEEE VTS. He is fellow of FIEEE, FIET, and EURASIP. In 2009 he was awarded the honorary doctorate Doctor Honoris Causa by the Technical University of Budapest and University of Edinburgh in 2015. His research is funded by the European Research Council's Senior Research Fellow Grant. He is fellow of FIEEE, FIET, and EURASIP. From 2008 to 2012, he was the Editor-in-Chief of the IEEE Press and a Chaired Professor also at Tsinghua University, Beijing.

AUTHOR QUERIES

AUTHOR PLEASE ANSWER ALL QUERIES

PLEASE NOTE: We cannot accept new source files as corrections for your paper. If possible, please annotate the PDF proof we have sent you with your corrections and upload it via the Author Gateway. Alternatively, you may send us your corrections in list format. You may also upload revised graphics via the Author Gateway.

AQ:1 = Please confirm/give details of funding source.
AQ:2 = Figs. 4 and 5 are not cited in body text. Please indicate where they should be cited.
AQ:3 = Please provide the author name for ref. [2].
AQ:4 = Please provide the page range for ref. [17].
AQ:5 = Please provide the volume no., issue no., page range, month, and year for ref. [82].